

**Prepared in cooperation with the Commonwealth of Massachusetts,
Massachusetts Geological Survey**

Bedrock Geologic Map of the Uxbridge Quadrangle, Worcester County, Massachusetts, and Providence County, Rhode Island

By Gregory J. Walsh

Pamphlet to accompany

Scientific Investigations Map 3295

U.S. Department of the Interior
SALLY JEWELL, Secretary

U.S. Geological Survey
Suzette M. Kimball, Acting Director

U.S. Geological Survey, Reston, Virginia: 2014

For more information on the USGS—the Federal source for science about the Earth, its natural and living resources, natural hazards, and the environment, visit <http://www.usgs.gov> or call 1–888–ASK–USGS.

For an overview of USGS information products, including maps, imagery, and publications, visit <http://www.usgs.gov/pubprod>

To order this and other USGS information products, visit <http://store.usgs.gov>

Any use of trade, firm, or product names is for descriptive purposes only and does not imply endorsement by the U.S. Government.

Although this information product, for the most part, is in the public domain, it also may contain copyrighted materials as noted in the text. Permission to reproduce copyrighted items must be secured from the copyright owner.

Suggested citation:

Walsh, G.J., 2014, Bedrock geologic map of the Uxbridge quadrangle, Worcester County, Massachusetts, and Providence County, Rhode Island: U.S. Geological Survey Scientific Investigations Map 3295, 1 sheet, scale 1:24,000, 36-p. pamphlet, <http://dx.doi.org/10.3133/sim3295>.

ISSN 2329-132X

Contents

Introduction.....	1
Age of the Rocks/Stratigraphy.....	1
Metasedimentary Rocks of the Blackstone Group.....	1
Neoproterozoic Intrusive Rocks.....	2
Granitic Gneiss.....	2
Tonalite and Granodiorite Gneiss.....	8
Ironstone Quartz Diorite of Emerson (1917).....	9
Geochemistry.....	10
Results.....	10
Structural Geology.....	20
Ductile Structures.....	20
Relict Deformation (D_1).....	20
Second Generation Deformation (D_2).....	21
Third Generation Deformation (D_3).....	23
Fourth Generation Deformation (D_4).....	24
Comment on the Hope Valley Shear Zone.....	27
Brittle Structures.....	28
Brittle Faults.....	31
Metamorphism.....	31
Economic Geology.....	32
Acknowledgments.....	33
References Cited.....	33

Figures

1. Photographs showing the Blackstone Group migmatitic plagioclase porphyroblast gneiss adjacent to the Ironstone quartz diorite of Emerson (1917).....	2
2. Photographs showing contact relationships in the granitic gneisses of the Uxbridge quadrangle.....	4
3. Photographs of the fine-grained biotite granite gneiss of the Northbridge Granite Gneiss.....	5
4. Photographs showing the textural differences between the Ponaganset Gneiss and the Northbridge Granite Gneiss.....	6
5. Photographs of the tonalite gneiss showing the strongly lineated L-tectonite fabric viewed from two different directions.....	8
6. Photographs of the Ironstone quartz diorite of Emerson (1917), taken in the adjoining Blackstone quadrangle.....	9
7. Major and trace element discrimination diagrams for rock samples from the Uxbridge quadrangle.....	10
8. Trace and rare earth element discrimination diagrams for rock samples from the Uxbridge quadrangle.....	11

9. Photographs and sketch of relict S_1 foliation and F_2 folds in rocks of the Blackstone Group	20
10. Summary diagrams of D_2 and D_3 ductile structures.....	21
11. Photographs showing variation in the S_2 foliation in granitic rocks	22
12. Photographs showing S_3 mylonite zones and shear bands.....	23
13. Photograph showing syntectonic and post-tectonic hornblende.....	24
14. Summary diagrams showing the orientation of quartz veins and pegmatite dikes	25
15. Photographs of quartz veins and pegmatite dikes.....	26
16. Stereonets and rose diagrams of fractures.....	29
17. Photograph showing three main categories of fractures	30
18. Stereonet showing results of brittle fault inversion analysis.....	31
19. Photographs of the abandoned Scadden Silver Mine	32

Tables

1. Petrographic modes of selected rocks from the Ponaganset Gneiss.....	3
2. Petrographic modes of selected rocks from the Northbridge Granite Gneiss	7
3. Petrographic modes of selected rocks from the tonalite to granodiorite gneiss at Uxbridge	8
4. Petrographic modes of selected rocks from the Ironstone quartz diorite of Emerson (1917).....	9
5. Major, trace, and rare earth element whole-rock geochemistry from the Uxbridge quadrangle.....	12
6. Summary of foliation-parallel parting fractures by formation and rock type.....	28

Conversion Factors and Datums

Multiply	By	To obtain
	Length	
centimeter (cm)	0.3937	inch
meter (m)	3.281	foot (ft)
kilometer (km)	0.6214	mile (mi)
	Mass	
pound, avoirdupois (lb)	0.4536	kilogram (kg)

Vertical coordinate information is referenced to the National Geodetic Vertical Datum of 1929 (NGVD 29).

Horizontal coordinate information is referenced to the North American Datum of 1927 (NAD 27).

Bedrock Geologic Map of the Uxbridge Quadrangle, Worcester County, Massachusetts, and Providence County, Rhode Island

By Gregory J. Walsh¹

Introduction

The bedrock geology of the Uxbridge quadrangle consists of Neoproterozoic metamorphic and igneous rocks of the Avalon zone (Zen and others, 1983). In this area, rocks of the Avalon zone lie within the core of the Milford antiform, south and east of the terrane-bounding Bloody Bluff fault zone (fig. A on map) (Goldsmith, 1991c). Permian pegmatite dikes and quartz veins occur throughout the quadrangle. The oldest metasedimentary rocks include the Blackstone Group, which represents a Neoproterozoic peri-Gondwanan marginal shelf sequence. The metasedimentary rocks are intruded by Neoproterozoic arc-related plutonic rocks of the Rhode Island batholith (Zen and others, 1983; Zartman and Naylor, 1984; Bailey and others, 1989; Rast and Skehan, 1990; Skehan and Rast, 1990, 1995; Goldsmith, 1991a; Hermes and Zartman, 1992; Hibbard and others, 2006; Thompson and others, 2012).

The bedrock is overlain by Pleistocene to Quaternary alluvial deposits, stratified glacial deposits, areas of thick till in drumlins or drumlinoids, and thin till (Stone and others, 2008). The northwestern corner of the map area is underlain by a considerable amount of exposed bedrock. Elsewhere in the quadrangle, however, the bedrock is less well-exposed.

Previous mapping in the area is limited, and unpublished reconnaissance mapping at 1:24,000-scale by H.R. Dixon and Richard Goldsmith was the primary source of geologic data compiled on the 1:250,000-scale geologic map of Massachusetts (Zen and others, 1983) (hereinafter referred to as the State map). In addition to the information on the State map, much of the work by Goldsmith is contained in several important regional papers that followed the publication of the State map (Goldsmith, 1991a,b,c; Wones and Goldsmith, 1991). Early work described the regional geology and economic deposits (Jackson, 1840; Emerson and Perry, 1907; Emerson, 1917; Dale, 1908, 1923; and Pearre, 1956).

Mapping at 7.5-minute scales in adjacent quadrangles includes work in Grafton (Walsh and others, 2011),

Milford (Kopera and others, 2007), Oxford (Barosh, 2005), Thompson (Dixon, 1974), Chepachet (Quinn, 1967), Blackstone (Kopera and Shaw, 2008; McKniff, 1964), and Georgiaville (Richmond, 1952).

Age of the Rocks / Stratigraphy

The metamorphic and igneous rocks in the Uxbridge quadrangle are largely Neoproterozoic in age. Ages in this report conform to the time scale of Gradstein and others (2004). The oldest rocks in the quadrangle belong to the metasedimentary Blackstone Group. Historically the age of the Blackstone Group has been considered Neoproterozoic based on crosscutting Neoproterozoic intrusive rocks in the Avalon zone (Zen and others, 1983; Zartman and Naylor, 1984; Bailey and others, 1989; Goldsmith, 1991a; Hermes and others, 1994; Skehan and Rast, 1990, 1995). The Blackstone Group rocks are cut by the intrusive rocks of the Rhode Island batholith (Goldsmith, 1991a). Based on ages obtained from the adjacent Grafton quadrangle (Walsh and others, 2011), the granitic gneisses of the Uxbridge quadrangle range in age from about 612 to 606 Ma (mega-annum).

Metasedimentary Rocks of the Blackstone Group

Large discontinuous screens of biotite schist and quartzite of the Blackstone Group (Zb) occur in the southeastern part of the Uxbridge quadrangle. Minor amounts of calc-silicate rock and tremolite schist are also present. The distribution of schist and quartzite is quite variable and the two rock types could not be mapped separately. Schist and quartzite are present at virtually every outcrop. Locally, quartzite outcrops predominate and in these places only small amounts of schist are exposed. Large outcrops clearly show that the two rocks types are interbedded. Quartzite layers range from several centimeters to several meters thick; true thickness is locally duplicated where the rocks are isoclinally folded. The Blackstone Group locally contains calc-silicate rocks, and those locations are indicated as points on the map because

¹U.S. Geological Survey, Montpelier, VT 05601.

their extent and distribution were not mappable into separate polygons. New mapping confirms the distribution as depicted at State-map scales as either Blackstone Group undivided (unit Zb of Zen and others, 1983; Goldsmith, 1991a), Blackstone Group undifferentiated (unit Zbu of Hermes and others, 1994), or Blackstone Series undifferentiated (unit b of Quinn, 1971). Unit Zb in the Uxbridge quadrangle correlates with the Blackstone Series quartz-biotite schist (unit bb) of Richmond (1952) and McKniff (1964), and with the undivided Blackstone Series (unit bs) of Quinn (1967). Mapping partly supports the assertion by Goldsmith (1991a, p. E8) that “west of Blackstone, the Blackstone Group is difficult to divide because outcrops are poor and quartzite and amphibolite are extensively interlayered.” This statement is true with the exception that amphibolite was not observed in the Blackstone Group within the Uxbridge quadrangle, but was seen at one place in the migmatitic gneiss unit (Zbm) adjacent to the Ironstone quartz diorite of Emerson (1917) (Ziqd) in the neighboring Blackstone quadrangle.

In the southeastern corner of the map area, the Blackstone Group contains migmatitic plagioclase porphyroblast gneiss (unit Zbm; fig. 1). The migmatitic gneiss is distributed around the Ironstone quartz diorite suggesting that its formation is related to the intrusion. McKniff (1964, p. 8) noted the same type of rock in the area around the Ironstone type locality, in the adjoining Blackstone quadrangle where he described the rock as having “been soaked by granitic material.”

Neoproterozoic Intrusive Rocks

Granitic Gneiss

The majority of the quadrangle is underlain by Neoproterozoic intrusive rocks which occur in three categories: granitic gneiss, tonalitic gneiss, and minor amounts of quartz diorite.

The granitic gneisses include the equigranular Hope Valley Alaskite Gneiss, the megacrystic Ponaganset Gneiss, and the equigranular to megacrystic Northbridge Granite Gneiss. The latter two occur as large sheet-like bodies whose geometry was probably produced by a combination of the original tabular nature of the intrusions and the subsequent penetrative deformation. In this study, we use the nomenclature and ages of Walsh and others (2011) for the granitic gneisses. The Hope Valley Alaskite Gneiss is quite limited in the Uxbridge quadrangle, occurring mostly as dikes or sills. Two small map units of Hope Valley Alaskite Gneiss occur within the Northbridge Granite Gneiss along Route 146. The Hope Valley Alaskite Gneiss yielded a Sensitive High Resolution Ion Microprobe (SHRIMP) U-Pb zircon age of 606 ± 5 Ma from the adjacent Grafton quadrangle (Walsh and others, 2011). The Ponaganset Gneiss is widespread in the Uxbridge quadrangle and it maps continuously into the Grafton quadrangle, where it yielded a SHRIMP U-Pb zircon age of 612 ± 5 Ma (Walsh and others, 2011). Modes of the Ponaganset Gneiss are shown in table 1.



UX-1199_03.JPG



UX-1199_04.JPG



UX-1199_06.JPG

Figure 1. Photographs showing the Blackstone Group migmatitic plagioclase porphyroblast gneiss (Zbm) adjacent to the Ironstone quartz diorite of Emerson (1917) (Ziqd). A, Light-colored tonalitic to granitic leucosome in gray gneiss; B, Xenolith of quartzite (arrow); C, Dark paleosome, consisting largely of biotite schist with minor amounts of amphibolite and calc-silicate, invaded by lighter leucosome. Filenames, on this and subsequent figures, correspond to georeferenced station locations shown in the accompanying GIS database.

Table 1. Petrographic modes of selected rocks from the Ponaganset Gneiss.

[—, no data; tr, trace; Cz, clinozoisite; Q, P, and A: normalized quartz (Q), plagioclase (P), and alkali feldspar (A) for the International Union of Geological Sciences (IUGS) rock classification]

Sample no.	UX-1043	UX-1087	UX-1179	UX-1231	UX-1232	UX-1237	Total or average
Points counted	396	435	388	343	462	371	2,395
Zpg—Megacrystic biotite granite gneiss, in percent							
Quartz	36	30	31	28	34	36	33
Plagioclase	34	34	21	36	36	30	32
Alkali feldspar	20	30	30	21	19	26	24
Biotite	9	6	15	12	8	8	10
Muscovite	—	—	tr	—	tr	—	tr
Epidote/Cz	1	tr	1	2	2	tr	1
Hornblende	1	tr	—	1	1	tr	tr
Chlorite	—	—	—	—	tr	tr	tr
Opaque	tr	—	—	—	—	—	tr
Hematite	—	—	—	—	—	—	—
Titanite	tr	—	tr	tr	—	—	tr
Apatite	—	—	—	—	—	—	tr
Allanite	tr	—	—	—	—	—	tr
Garnet	—	—	—	—	—	—	—
Zircon	—	—	—	—	—	—	—
Totals	101	100	98	100	100	100	100
Q	41	32	38	33	38	39	33
P	37	36	26	42	40	33	40
A	22	32	36	25	22	28	27

Sample no.	UX-1042	UX-1082	UX-1092	Total or average
Points counted	396	391	419	1,206
Zphg - Megacrystic hornblende-biotite granite gneiss, in percent				
Quartz	29	35	40	35
Plagioclase	32	35	23	30
Alkali feldspar	35	13	21	23
Biotite	1	13	10	8
Muscovite	—	tr	—	tr
Epidote/Cz	tr	3	2	2
Hornblende	2	tr	4	2
Chlorite	—	tr	—	tr
Opaque	—	tr	—	tr
Hematite	—	—	—	—
Titanite	1	tr	—	tr
Apatite	1	—	—	tr
Allanite	—	—	tr	tr
Garnet	—	—	—	—
Zircon	—	—	—	—
Totals	101	99	100	100
Q	30	42	48	40
P	33	42	27	34
A	37	16	25	26

4 Bedrock Geologic Map of the Uxbridge Quadrangle, Worcester County, Massachusetts, and Providence County, Rhode Island

The Northbridge Granite Gneiss is also widespread in the Uxbridge quadrangle, and in the Grafton quadrangle it yielded a SHRIMP U-Pb zircon age of 607 ± 5 Ma (Walsh and others, 2011). Field evidence shows that biotite granite gneiss of the

Northbridge Granite Gneiss (Zncg) intrudes the Ponaganset Gneiss (Zpg), and both units are cut by dikes or sills of the Hope Valley Alaskite Gneiss (Zhv) (fig. 2). The overlapping U-Pb zircon ages and the chemical similarity between the

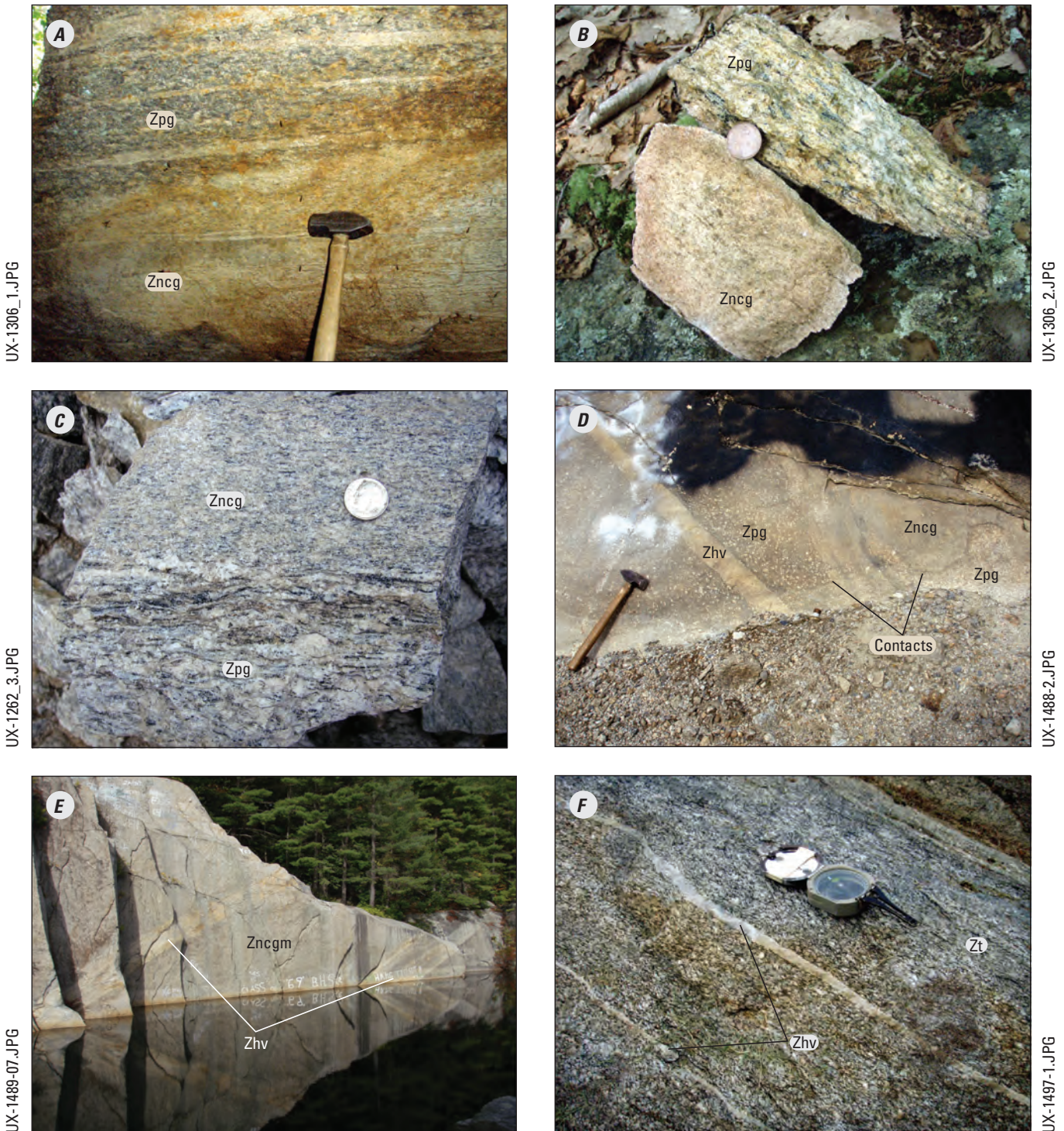


Figure 2. Photographs showing contact relationships in the granitic gneisses of the Uxbridge quadrangle. *A*, Ponaganset Gneiss (Zpg) with multiple sills of Northbridge Granite Gneiss (Zncg); *B*, Hand samples of rocks in *A*; *C*, Block showing sharp contact between Zpg and Zncg; *D*, Zpg with folded layer of Zncg and thin dike of Hope Valley Alaskite Gneiss (Zhv); *E*, Two sills of alaskite (Zhv) in the Northbridge Granite Gneiss (Zncgm) in an abandoned granite quarry on Quarry Hill; and *F*, Two thin sills of alaskite (Zhv) in the tonalite and granodiorite gneiss (Zt).

Northbridge Granite Gneiss and the Hope Valley Alaskite Gneiss suggest that they are related to the same plutonic event (Walsh and others, 2011). Chemical data presented below further support this conclusion. The fine-grained biotite granite gneiss of the Northbridge Granite Gneiss (Znfg) has not been dated, but xenoliths of Znfg within the coarse-grained biotite granite gneiss (Znbg) show that it must be older (fig. 3). Cross-cutting relationships of the megacrystic biotite granite gneiss

(Znbgm) of the Northbridge Granite Gneiss with its adjacent units were not directly observed in the field. The texture and map distribution of the Znbgm unit suggests that it represents a transitional rock between the equigranular coarse-grained biotite granite gneiss of the Northbridge Granite Gneiss (Znbg) and the distinctly megacrystic biotite granite gneiss of the Ponaganset Gneiss (Zpg) (fig. 4). Modes of the Northbridge Granite Gneiss are shown in table 2.

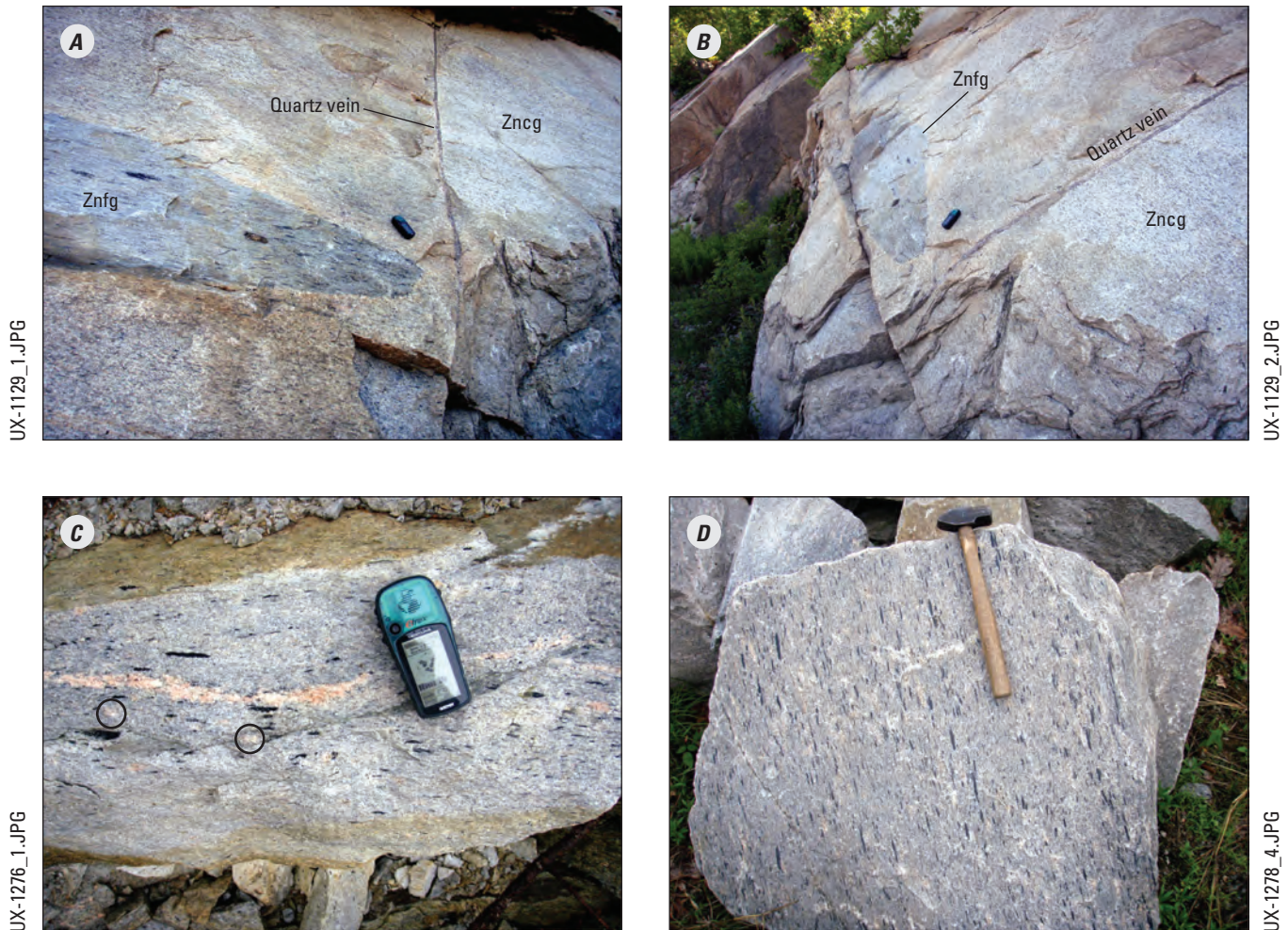


Figure 3. Photographs of the fine-grained biotite granite gneiss (Znfg) of the Northbridge Granite Gneiss. The GPS receiver in *A*, *B*, and *C* is 10.5 cm long. *A* and *B*, Equigranular coarse-grained biotite granite gneiss (Znbg) with xenolith of Znfg, shown from two perspectives; *C*, Downplunge view showing characteristic biotite streaks, pink potassium (K-) feldspar segregations, and small (<1 cm) K-feldspar augen (circled); *D*, Block showing characteristic biotite aggregate lineation (parallel to hammer handle) on the foliation surface.

Figure 4. Photographs showing the textural differences between the Ponaganset Gneiss (Zpg) and the Northbridge Granite Gneiss. *A*, Megacrystic biotite granite gneiss of the Ponaganset Gneiss (Zpg); *B*, Inequigranular megacrystic biotite granite gneiss of the Northbridge Granite Gneiss (Zncgm); *C*, Equigranular biotite granite gneiss of the Northbridge Granite Gneiss (Zncg). The Zncgm unit in *B* is a transitional rock between the megacrystic (Zpg) and equigranular (Zncg) end members. Arrow near top of *A* shows the end of a pen for scale (1 cm diameter). Arrow in *B* shows a quartz vein (gray) with a median line of alkali feldspar.



Table 2. Petrographic modes of selected rocks from the Northbridge Granite Gneiss.

[—, no data; tr, trace; Cz, clinozoisite; incl., including; Mt, magnetite; Q, P, and A: normalized quartz (Q), plagioclase (P), and alkali feldspar (A) for the International Union of Geological Sciences (IUGS) rock classification]

Sample no.	UX-1001	UX-1025	UX-1105	UX-1121A	UX-1291	UX-1587	Total or average
Points counted	397	427	426	492	389	580	2,711
Zncg - Coarse-grained biotite granite gneiss, in percent							
Quartz	42	27	31	29	34	45	35
Plagioclase	20	37	31	43	33	30	33
Alkali feldspar	33	33	27	21	29	18	26
Biotite	6	4	3	2	4	7	4
Muscovite	—	—	6	4	tr	tr	2
Epidote/Cz	tr	tr	tr	tr	tr	tr	tr
Hornblende	—	—	—	—	—	—	—
Chlorite	tr	tr	1	tr	tr	tr	tr
Opaque incl. Mt	tr	tr	tr	tr	tr	tr	tr
Hematite	—	—	—	tr	—	—	tr
Titanite	—	tr	—	—	tr	—	tr
Apatite	—	tr	—	tr	—	tr	tr
Allanite	—	—	—	—	tr	—	tr
Garnet	—	tr	—	tr	—	—	tr
Zircon	—	—	—	—	—	—	—
Totals	101	101	99	99	100	100	100
Q	44	28	34	31	36	48	37
P	21	38	35	46	35	32	35
A	35	34	31	22	30	20	28

Sample no.	UX-1001A	UX-1157A	UX-1425	UX-1528	Total or average
Points counted	420	386	406	423	1,635
Zncgm - Megacrystic biotite granite gneiss, in percent					
Quartz	29	32	37	30	32
Plagioclase	39	34	30	44	37
Alkali feldspar	24	24	29	20	24
Biotite	6	9	4	3	5
Muscovite	—	1	tr	1	tr
Epidote/Cz	tr	1	tr	tr	tr
Hornblende	—	—	—	—	—
Chlorite	tr	tr	—	tr	tr
Opaque incl. Mt	2	tr	tr	1	1
Hematite	—	—	—	tr	tr
Titanite	—	—	tr	—	tr
Apatite	tr	tr	—	—	tr
Allanite	—	—	—	tr	tr
Garnet	—	—	—	—	—
Zircon	—	—	—	—	—
Totals	100	101	100	99	99
Q	31	36	38	32	34
P	43	38	31	47	40
A	26	27	30	21	26

Tonalite and Granodiorite Gneiss

Tonalitic gneiss crops out along the eastern border of the quadrangle and in several smaller plutonic bodies in the southeastern part of the map area. The rocks are informally named the “tonalite to granodiorite gneiss at Uxbridge” for the main unit (Zt) exposed in Uxbridge. The type locality is an abandoned quarry along Granite Street on the eastern border of the map. The rock is characteristically salt and pepper colored and may contain a well-developed lineation or L-tectonite fabric (fig. 5). The rock intrudes the Blackstone Group rocks and is intruded by alaskite dikes. Contacts with the adjacent plutonic

rocks are not exposed. The rock may be an older, more mafic phase of the Ponaganset Gneiss. Modes are shown in table 3.

Emerson (1917) described this rock as a border phase of the Milford granite, and suggested that it was part of the Ironstone quartz diorite. More detailed work in the southern part of the Blackstone quadrangle (McKniff, 1964) showed that the quartz diorite was not a border phase of either the Milford or Esmond Granites, but predated the granitic plutons. The eastern extent of the tonalitic rock, however, has not been mapped in the western part of the Blackstone quadrangle (McKniff, 1964; Koper and Shaw, 2008), so its relationship to the Milford Granite remains uncertain.

Table 3. Petrographic modes of selected rocks from the tonalite to granodiorite gneiss at Uxbridge (Zt).

[—, no data; Cz, clinozoisite; tr, trace; incl., including; Mt, magnetite; Q, P, and A: normalized quartz (Q), plagioclase (P), and alkali feldspar (A) for the International Union of Geological Sciences (IUGS) rock classification]

Sample no.	UX-1569	UX-1016	UX-1148	UX-1398	UX-1004	Total or average
Points counted	225	631	364	409	391	2,020
Percent						
Quartz	19	35	33	26	25	29
Plagioclase	32	41	43	52	52	45
Alkali feldspar	1	7	6	4	4	5
Biotite	22	12	8	14	14	13
Muscovite	—	3	1	—	—	1
Epidote/Cz	8	tr	2	2	2	2
Hornblende	15		6	1	3	4
Chlorite	1	2	—	—	tr	1
Opaque incl. Mt	—	—	—	—	—	—
Hematite	—	—	—	—	—	—
Titanite	2	—	—	tr	tr	tr
Apatite	tr	tr	tr	tr	1	tr
Allanite	—	tr	—	tr	—	tr
Garnet	—	—	—	—	—	—
Zircon	—	—	—	—	—	—
Totals	100	100	99	99	101	100
Q	37	42	40	32	31	37
P	61	50	53	63	64	57
A	2	8	8	5	5	6



Figure 5. Photographs of the tonalite gneiss (Zt) showing the strongly lineated L-tectonite fabric viewed from two different directions. *A*, Perpendicular to the lineation; *B*, Parallel to the lineation, looking up plunge. Note the alkali feldspar megacrysts circled in *B*.

UX-1015_1.JPG

UX-1015_2.JPG

Ironstone Quartz Diorite of Emerson (1917)

The Ironstone quartz diorite (Ziqd) crops out along the southeastern border of the quadrangle and extends into the adjacent Blackstone quadrangle (McKniff, 1964). The rock is equigranular and consists largely of biotite, quartz, plagioclase, and hornblende (fig. 6). Plagioclase is partly replaced by epidote. It was named by Emerson (1917, p. 168) for a “black, heavy rock” exposed near the village of Ironstone, in the adjacent Blackstone quadrangle about 1 km east of the quadrangle border with Uxbridge. At Ironstone, where the rock is well exposed along Elmwood Avenue, just west of Route 146 in the town of Uxbridge, a roadcut contains darker enclaves enclosed in lighter colored rock having distinct, leucocratic quartz-plagioclase



UX-1205_1.JPG



UX-1618_5.JPG

Figure 6. Photographs of the Ironstone quartz diorite of Emerson (1917) (Ziqd), taken in the adjoining Blackstone quadrangle. *A*, Equigranular rock exposed north of East Ironstone Road; *B*, Darker, more mafic enclaves within lighter colored, more felsic rock along Elmwood Avenue at the type locality.

aggregates (fig. 6*B*). The Ironstone intrudes the biotite schist and quartzite of the Blackstone Group, and is in turn intruded by dikes of biotite granite gneiss. Modes are shown in table 4.

Mapping in the Uxbridge quadrangle shows that the Ironstone is not a border phase of the granitic gneiss called Milford Granite by Emerson (1917), but instead is an older, more mafic pluton, that predates the granitic gneiss now mapped as Northbridge. Chemically one sample (UX-1618), collected from the type locality 1 km east of the quadrangle boundary, is a gabbro (table 5). The sample location is not shown on the map but is included in the GIS database. The Ironstone quartz diorite is surrounded by migmatitic gneiss whose protolith includes the Blackstone Group rocks (fig. 1).

Table 4. Petrographic modes of selected rocks from the Ironstone quartz diorite of Emerson (1917) (Ziqd).

[—, no data; Cz, clinzoisite; tr, trace; Q, P, and A: normalized quartz (Q), plagioclase (P), and alkali feldspar (A) for the International Union of Geological Sciences (IUGS) rock classification]

Sample no.	UX-1202	UX-1207	UX-1617	UX-1618	Total or average
Points counted	396	385	407	402	1,590
	Percent				
Quartz	18	7	11	9	11
Plagioclase	42	32	18	13	27
Alkali feldspar	—	—	—	—	—
Biotite	8	1	14	5	7
Muscovite	—	—	—	—	—
Epidote/Cz	1	1	1	tr	1
Hornblende	30	59	55	65	52
Chlorite	—	—	tr	—	tr
Magnetite	—	—	—	—	—
Opaque	—	—	tr	5	1
Hematite	—	—	—	—	—
Titanite	—	—	—	—	—
Apatite	tr	tr	—	1	tr
Clinzoisite	—	—	—	—	—
Allanite	—	—	—	—	—
Garnet	—	—	—	—	—
Zircon	—	—	—	—	—
Totals	99	100	99	98	99
Q	29	17	38	41	28
P	71	83	63	59	72
A	0	0	0	0	0

Geochemistry

Thirty intrusive rock samples were analyzed for major, trace, and rare earth elements (REE). Geochemistry data are located in table 5 and in the GIS database, and results are plotted in figures 7 and 8. Geochemical analyses were conducted by SGS Minerals, Toronto, Ontario, Canada. Major elements were analyzed by X-ray fluorescence using lithium metaborate fused disks (SGS Minerals Method XRF76S). Trace elements and REE were analyzed by inductively coupled plasma-mass spectrometry using sodium peroxide fusion (SGS Minerals Method ICM90A).

Results

The granitic gneisses are calc-alkaline granites (fig. 7A, B). They are mildly peraluminous, with the Ponaganset Gneiss plotting along the metaluminous-peraluminous boundary

(fig. 7C). The more mafic rocks are tholeiitic tonalites to granodiorites (fig. 7A, B), and they are largely metaluminous with one sample plotting in the peraluminous field (fig. 7C). The Rb versus Y+Nb tectonic discrimination diagram (fig. 7D) shows the granitic rocks as volcanic-arc to within-plate granites, and the more mafic rocks as volcanic-arc granites. Chondrite-normalized REE patterns and multi-element “spider diagrams” (fig. 8A–D) are consistent with leucocratic continental rocks showing both crust and mantle sources (Thompson and others, 1984). The Ponaganset Gneiss and the intermediate to mafic rocks show more primitive signatures, suggesting less contamination from continental crust or sediments. Most granitic samples have fairly steep abundances of light rare earth elements (LREE), with normalized La values ranging from about 80 to 300, and relatively flat abundances of heavy rare earth elements (HREE) (fig. 8C). Two samples of the Northbridge Granite Gneiss (unit Zncg) show depleted LREE (fig. 8C), possibly related to the fractional crystallization of allanite (Thompson and others, 1984). Prominent negative Eu

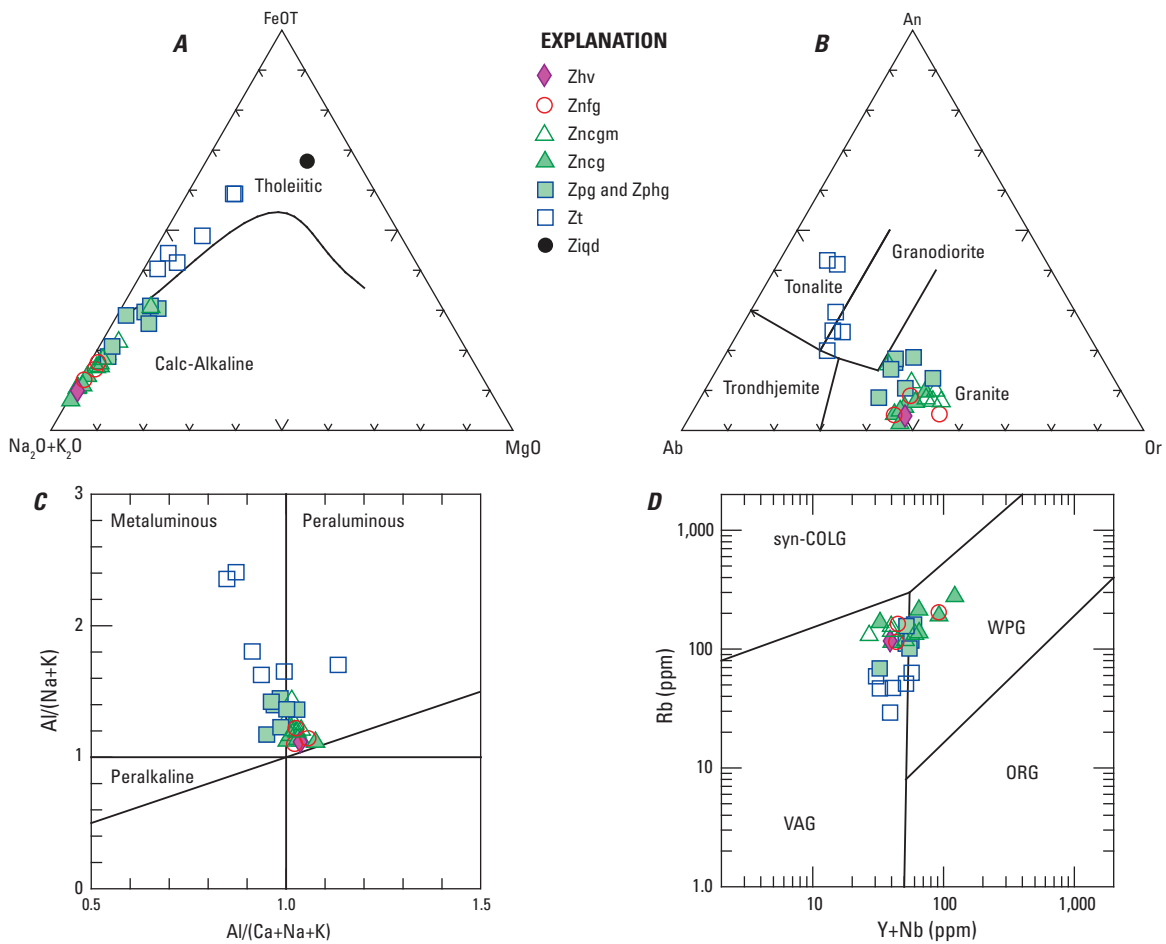


Figure 7. Major and trace element discrimination diagrams for rock samples from the Uxbridge quadrangle. A, $\text{Na}_2\text{O} + \text{K}_2\text{O} - \text{FeOT} - \text{MgO}$ (AFM) diagram, modified from Irvine and Baragar (1971). B, Normative An-Ab-Or (anorthite-albite-orthoclase) classification diagram modified from O'Connor (1965) and Barker (1979). C, Alumina saturation diagram modified from Shand (1951) and Maniar and Piccoli (1989). D, Tectonic discrimination diagram modified from Pearce and others (1984). VAG, volcanic arc granites; ORG, ocean ridge granites; WPG, within-plate granite; syn-COLG, syn-collisional granites. See text for discussion. ppm, parts per million.

anomalies are present in all granitic samples from the Northbridge Granite Gneiss and Hope Valley Alaskite Gneiss, but are less pronounced in the Ponaganset Gneiss samples (fig. 8A, C), suggesting greater fractional crystallization of plagioclase in the more leucocratic rocks. The intermediate to mafic rocks show fairly moderate LREE abundances with normalized La values ranging from about 80 to 400, and have relatively flat HREE (fig. 8A). Eu anomalies are absent to slightly positive in the intermediate to mafic samples (fig. 8A). The spider diagrams for the granitic Northbridge Granite Gneiss and Hope Valley Alaskite Gneiss samples are similar, showing enrichment in

Rb, Th, and K, with negative Nb, Sr, P, and Ti anomalies that are characteristic of continental granites (fig. 8D). The samples of the granitic Ponaganset Gneiss show similar trends to the other granitic rocks, but less pronounced anomalies. The intermediate to mafic rocks show even less pronounced anomalies, suggesting greater proportion of a mantle source (fig. 8B). The U/Th ratios are quite similar to those reported by Wones and Goldsmith (1991) for similar rocks in the Milford antiform, with the exception of three samples of the Northbridge Granite Gneiss (unit Zncg) that have slightly higher values of Th and higher values of U (fig. 8E).

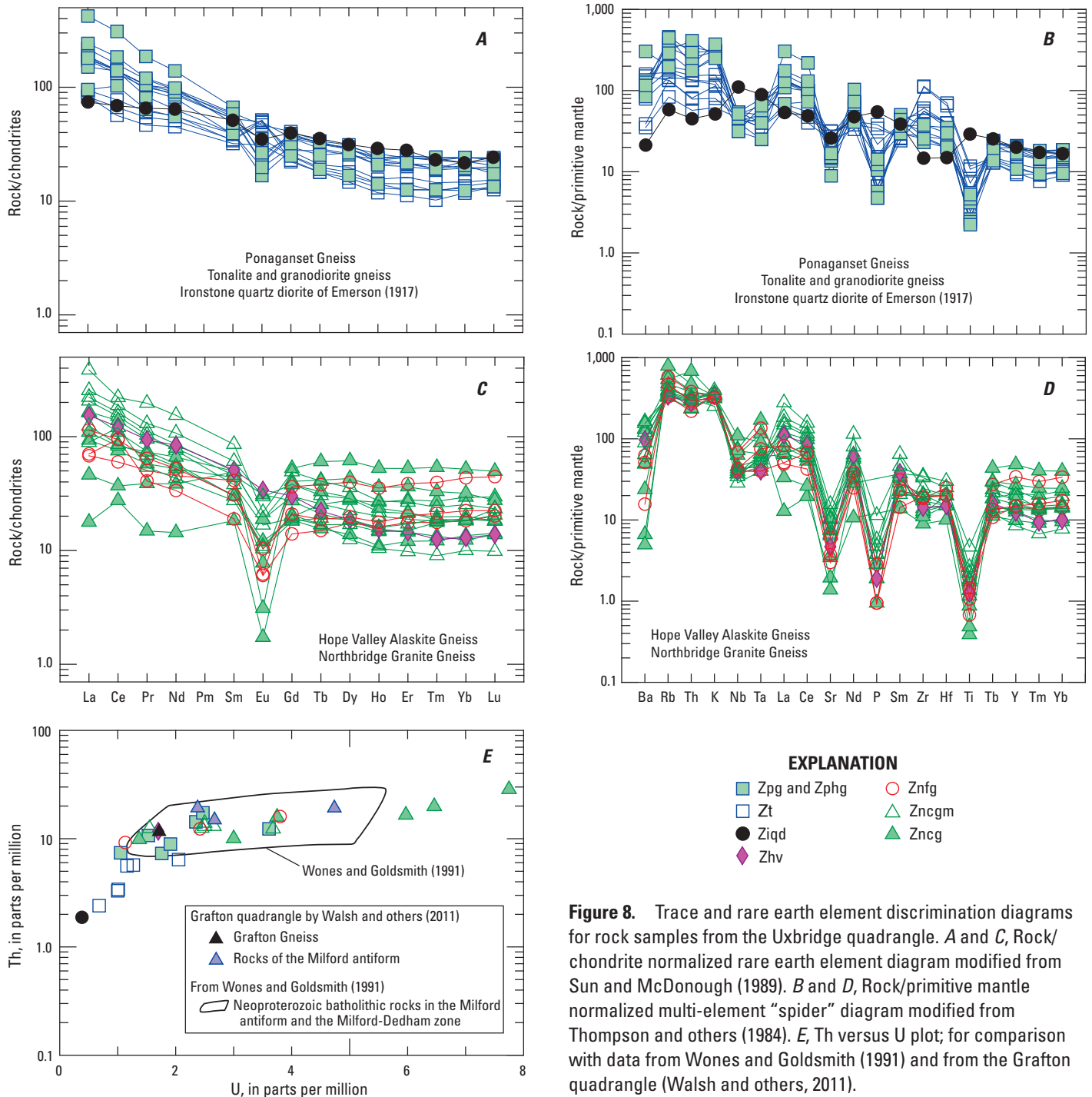


Figure 8. Trace and rare earth element discrimination diagrams for rock samples from the Uxbridge quadrangle. A and C, Rock/chondrite normalized rare earth element diagram modified from Sun and McDonough (1989). B and D, Rock/primitive mantle normalized multi-element “spider” diagram modified from Thompson and others (1984). E, Th versus U plot; for comparison with data from Wones and Goldsmith (1991) and from the Grafton quadrangle (Walsh and others, 2011).

Table 5. Major, trace, and rare earth element whole-rock geochemistry from the Uxbridge quadrangle.—Continued

[Geochemical analyses were conducted on 30 samples of intrusive rock by SGS Minerals, Toronto, Ontario, Canada. Major elements were analyzed by X-ray fluorescence (XRF) using lithium metaborate fused disks (SGS Minerals Method XRF76S). Trace and rare earth elements were analyzed by inductively coupled plasma-mass spectrometry (ICP-MS) using sodium peroxide fusion (SGS Minerals Method ICM90A). LOI, loss on ignition; ppm, parts per million]

Sample no.	GR-283	UX-1001-A	UX-1157-A	UX-1291	UX-1425	UX-1434	UX-1001
Map unit	Zn _{cg} m	Zn _{cg}					
Trace and rare earth elements (ppm)—Continued							
Cd	<0.2	<0.2	<0.2	<0.2	<0.2	<0.2	<0.2
Ce	99.6	92.2	115	135	73.6	52.3	67
Co	2.6	1.8	4.4	1.6	1.4	1.4	2
Cs	1	2.8	2.3	1.1	1.3	1.2	2.4
Dy	5.68	3.16	7.25	9.07	4.74	4.3	3.51
Er	3.12	1.62	3.51	4.4	2.83	2.47	1.99
Eu	1.09	0.97	1.72	1.25	0.6	0.63	0.7
Ga	16	14	17	16	15	14	14
Gd	6.15	3.95	7.85	10.1	3.72	4.22	3.8
Ge	1	1	2	2	1	1	2
Hf	6	3	5	4	4	4	3
Ho	1.13	0.59	1.23	1.54	0.9	0.83	0.62
In	<0.2	<0.2	<0.2	<0.2	<0.2	<0.2	<0.2
La	52.6	48.8	60.3	91.4	21.1	29.4	38.4
Lu	0.46	0.25	0.46	0.59	0.59	0.52	0.36
Mo	<2	<2	<2	<2	<2	<2	<2
Nb	13	10	16	14	12	13	13
Nd	40	35.4	50.2	71.9	20.1	25.5	27
Pb	16	14	17	12	16	16	23
Pr	10.7	9.83	12.4	18.7	5.12	6.55	7.04
Rb	115	130	118	133	155	141	167
Sb	<0.1	<0.1	<0.1	<0.1	<0.1	<0.1	<0.1
Sm	7.6	5.8	9.3	13.1	4.2	4.6	4.6
Sn	4	1	1	2	1	2	2
Ta	0.9	0.8	1.1	1	1.2	1.1	1.3
Tb	0.96	0.63	1.14	1.52	0.72	0.63	0.58
Th	12.5	12.3	13	13	12.4	13.9	15.8
Tl	<0.5	0.6	<0.5	0.6	0.6	0.6	0.7
Tm	0.46	0.23	0.5	0.61	0.48	0.45	0.31
U	2.45	3.68	2.5	2.66	1.55	2.5	3.75
W	<1	<1	<1	<1	<1	<1	<1
Y	31.3	17	35.2	46.4	27.8	26.9	19.7
Yb	3.2	1.7	3.4	4.3	3.1	3.1	2.3
Zr	238	140	227	168	134	140	118

Table 5. Major, trace, and rare earth element whole-rock geochemistry from the Uxbridge quadrangle.—Continued

[Geochemical analyses were conducted on 30 samples of intrusive rock by SGS Minerals, Toronto, Ontario, Canada. Major elements were analyzed by X-ray fluorescence (XRF) using lithium metaborate fused disks (SGS Minerals Method XRF76S). Trace and rare earth elements were analyzed by inductively coupled plasma-mass spectrometry (ICP-MS) using sodium peroxide fusion (SGS Minerals Method ICM90A). LOI, loss on ignition; ppm, parts per million]

Sample no.	UX-1025	UX-1025	UX-1105	UX-1116	UX-1121-A	UX-1004	UX-1016	UX-1112
Map unit	Zn _{cg}	Zt	Zt	Zt				
Trace and rare earth elements (ppm)—Continued								
Cd	<0.2	<0.2	0.2	<0.2	<0.2	<0.2	<0.2	<0.2
Ce	16.8	22.6	46	84.6	50.6	81.3	34.6	47.3
Co	<0.5	<0.5	0.9	<0.5	<0.5	6.6	2.3	8.2
Cs	4.6	5.9	2.3	1.6	2.6	2.1	2.8	4.2
Dy	7.01	15.6	10.9	4.66	7.43	6.61	4.05	5.03
Er	4.62	8.7	6	2.4	3.59	3.33	2.09	2.68
Eu	0.1	0.18	0.45	1.79	1.09	2.88	1.8	2.84
Ga	16	21	16	15	17	18	14	19
Gd	4.05	10.8	8.32	5.62	7.76	7.4	4.7	5.66
Ge	2	2	1	1	2	2	1	1
Hf	2	4	3	3	3	8	8	14
Ho	1.5	2.98	2.03	0.85	1.33	1.17	0.74	0.88
In	<0.2	<0.2	<0.2	<0.2	<0.2	<0.2	<0.2	<0.2
La	4.2	10.9	22.1	39.2	25.9	40.8	19.7	22.3
Lu	0.75	1.26	0.7	0.35	0.47	0.48	0.32	0.39
Mo	<2	<2	<2	<2	<2	<2	<2	<2
Nb	22	26	38	15	25	19	14	16
Nd	6.7	17.9	24.4	37	30.9	41.5	21	26.3
Pb	19	20	19	17	21	8	12	8
Pr	1.41	3.68	5.48	9.04	6.97	9.44	4.42	5.83
Rb	213	276	190	114	137	51.1	46.7	47.1
Sb	<0.1	0.1	0.1	<0.1	0.1	<0.1	<0.1	<0.1
Sm	2.8	7.5	6.7	7	7.6	8.1	4.9	5.2
Sn	4	5	1	<1	1	<1	<1	<1
Ta	2.3	3.4	1.8	0.9	1.3	0.8	0.5	0.7
Tb	0.95	2.26	1.55	0.78	1.23	1.08	0.67	0.78
Th	16.5	19.8	28.5	9.8	10	5.7	3.4	3.3
Tl	0.9	1.2	0.8	<0.5	0.5	<0.5	<0.5	<0.5
Tm	0.69	1.37	0.84	0.34	0.47	0.48	0.32	0.37
U	5.97	6.46	7.75	1.37	3	1.27	1.01	1
W	<1	<1	<1	<1	1	<1	<1	<1
Y	42.8	96	54.3	25.2	40.1	32.7	18.6	25
Yb	5	8.8	5.4	2.1	3.2	3.3	2.2	2.5
Zr	61.1	81.9	94.7	87.4	74.9	414	381	774

Table 5. Major, trace, and rare earth element whole-rock geochemistry from the Uxbridge quadrangle.—Continued

[Geochemical analyses were conducted on 30 samples of intrusive rock by SGS Minerals, Toronto, Ontario, Canada. Major elements were analyzed by X-ray fluorescence (XRF) using lithium metaborate fused disks (SGS Minerals Method XRF76S). Trace and rare earth elements were analyzed by inductively coupled plasma-mass spectrometry (ICP-MS) using sodium peroxide fusion (SGS Minerals Method ICM90A). LOI, loss on ignition; ppm, parts per million]

Sample no.	UX-1134	UX-1148	UX-1398	UX-1042	UX-1043	UX-1082	UX-1087	UX-1092
Map unit	Zt	Zt	Zt	Zphg	Zpg	Zphg	Zpg	Zphg
Major elements (percent)								
SiO ₂	66.4	76.4	69.9	73.9	73.1	74.8	69.8	72
Al ₂ O ₃	13.6	11.9	13.9	13.6	13.1	12.4	14.4	13.7
Fe ₂ O ₃	7.92	3.93	5.38	2.23	3.55	2.33	4.16	3.95
MgO	1.2	0.26	0.74	0.35	0.6	0.28	0.99	0.69
CaO	5.47	2.61	3.46	1.49	2.27	1.36	2.57	2.53
Na ₂ O	2.85	3.25	3.71	4.19	3.2	3.27	3.1	3.28
K ₂ O	0.89	1.72	2.26	4.35	3.81	4.36	4.48	3.92
TiO ₂	1.11	0.33	0.54	0.27	0.43	0.25	0.57	0.48
P ₂ O ₅	0.36	0.07	0.16	0.06	0.11	0.05	0.15	0.13
MnO	0.19	0.1	0.13	0.04	0.07	0.05	0.08	0.08
Cr ₂ O ₃	<0.01	<0.01	<0.01	<0.01	<0.01	<0.01	<0.01	<0.01
LOI	0.43	0.39	0.28	0.3	0.2	0.18	0.38	0.25
Totals	100.4	101	100.5	100.8	100.4	99.3	100.7	101
Trace and rare earth elements (ppm)								
Ba	242	1,100	711	930	769	655	583	871
Be	<5	<5	<5	<5	<5	6	<5	<5
Ca	3.81	1.85	2.42	1.09	1.56	0.97	1.85	1.78
Cr	20	<10	<10	10	20	20	<10	10
Cu	<5	<5	<5	6	<5	9	<5	<5
Fe	5.51	2.68	3.78	1.51	2.45	1.69	2.92	2.66
K	0.75	1.36	1.79	3.46	2.96	3.49	3.51	3.06
Li	20	20	20	10	20	30	40	20
Mg	0.67	0.15	0.42	0.2	0.33	0.16	0.57	0.38
Mn	1,420	740	940	320	510	420	650	560
Ni	10	11	24	6	6	21	19	9
P	0.17	0.03	0.08	0.02	0.04	0.02	0.08	0.04
Sc	36	12	23	7	12	12	17	15
Sr	375	277	267	201	160	105	176	173
Ti	0.6	0.18	0.31	0.15	0.24	0.14	0.32	0.27
V	50	10	26	17	31	15	56	36
Zn	108	61	87	45	56	52	60	60
Ag	<1	<1	<1	<1	<1	<1	<1	<1
As	<5	<5	<5	<5	<5	<5	<5	<5
Bi	<0.1	<0.1	<0.1	0.6	<0.1	<0.1	<0.1	<0.1

Table 5. Major, trace, and rare earth element whole-rock geochemistry from the Uxbridge quadrangle.—Continued

[Geochemical analyses were conducted on 30 samples of intrusive rock by SGS Minerals, Toronto, Ontario, Canada. Major elements were analyzed by X-ray fluorescence (XRF) using lithium metaborate fused disks (SGS Minerals Method XRF76S). Trace and rare earth elements were analyzed by inductively coupled plasma-mass spectrometry (ICP-MS) using sodium peroxide fusion (SGS Minerals Method ICM90A). LOI, loss on ignition; ppm, parts per million]

Sample no.	UX-1134	UX-1148	UX-1398	UX-1042	UX-1043	UX-1082	UX-1087	UX-1092
Map unit	Zt	Zt	Zt	Zphg	Zpg	Zphg	Zpg	Zphg
Trace and rare earth elements (ppm)—Continued								
Cd	<0.2	<0.2	<0.2	<0.2	<0.2	<0.2	<0.2	<0.2
Ce	40.8	86.5	85.7	85	189	97.5	85.8	85.6
Co	8	2	4.9	2.8	4.3	1.8	7	4.8
Cs	2.3	1.4	1.5	2.2	2.2	1.4	5.1	1.6
Dy	4.57	3.73	7.91	6.48	7.42	7.56	7.28	7.22
Er	2.34	1.85	4	3.98	3.52	3.97	4.12	3.52
Eu	2.97	2.98	2.7	0.97	1.4	1.27	1.25	1.54
Ga	18	15	18	16	17	16	18	16
Gd	5.17	4.55	8.37	5.71	8.07	7.9	7.42	7.5
Ge	1	1	1	1	1	1	2	1
Hf	13	7	8	5	7	5	4	4
Ho	0.81	0.67	1.36	1.3	1.25	1.47	1.36	1.33
In	<0.2	<0.2	<0.2	<0.2	<0.2	<0.2	<0.2	<0.2
La	19.5	44.1	41.7	35.7	100	51.5	44.7	42.7
Lu	0.37	0.34	0.58	0.6	0.52	0.61	0.59	0.51
Mo	<2	<2	<2	<2	<2	<2	<2	<2
Nb	16	11	19	14	14	15	19	16
Nd	23.9	37.6	45.2	29.9	65	44.4	40	42.5
Pb	7	8	10	27	11	13	16	13
Pr	5.16	9.04	9.92	7.88	17.7	11.1	9.81	9.98
Rb	29.2	59	63.1	130	111	118	161	101
Sb	<0.1	<0.1	<0.1	<0.1	<0.1	<0.1	<0.1	<0.1
Sm	5.3	5.9	9.1	6	10.2	8.4	8.1	8.9
Sn	<1	<1	2	3	2	2	3	1
Ta	0.7	<0.5	1	1.5	0.9	1	1.6	0.8
Tb	0.74	0.67	1.26	1.04	1.2	1.19	1.18	1.24
Th	2.4	5.6	6.4	14.3	17.3	10.7	12.3	7.3
Tl	<0.5	<0.5	<0.5	0.6	<0.5	<0.5	0.7	<0.5
Tm	0.31	0.26	0.6	0.58	0.49	0.6	0.62	0.53
U	0.68	1.16	2.05	2.35	2.47	1.53	3.61	1.76
W	<1	<1	<1	<1	<1	<1	<1	<1
Y	23	19.5	38	39	37.4	41.8	40.5	38.9
Yb	2.3	2	3.7	4.1	3.8	4.1	4.1	3.3
Zr	756	381	358	187	252	211	157	185

Table 5. Major, trace, and rare earth element whole-rock geochemistry from the Uxbridge quadrangle.—Continued

[Geochemical analyses were conducted on 30 samples of intrusive rock by SGS Minerals, Toronto, Ontario, Canada. Major elements were analyzed by X-ray fluorescence (XRF) using lithium metaborate fused disks (SGS Minerals Method XRF76S). Trace and rare earth elements were analyzed by inductively coupled plasma-mass spectrometry (ICP-MS) using sodium peroxide fusion (SGS Minerals Method ICM90A). LOI, loss on ignition; ppm, parts per million]

Sample no. Map unit	UX-1179 Zpg	UX-1237 Zpg	UX-1122 Zhv	UX-1274 Znfg	UX-1276 Znfg	UX-1591 Znfg	UX-1618 Ziqd
Trace and rare earth elements (ppm)—Continued							
Cd	<0.2	<0.2	<0.2	<0.2	<0.2	<0.2	0.3
Ce	62.9	113	75	58.2	36.7	57.8	42.4
Co	6.7	1.6	<0.5	0.6	<0.5	1	54.6
Cs	4.1	1.3	1.7	1.1	1.4	3.3	1.4
Dy	6.74	4.26	4.75	4.43	10.1	5.01	8.02
Er	3.59	2.07	2.41	2.91	6.4	3.33	4.65
Eu	1.15	2.04	1.97	0.35	0.36	0.6	2.04
Ga	16	16	16	14	18	16	21
Gd	6.14	5.11	6.2	2.87	7.46	4.28	8.19
Ge	1	1	1	1	2	2	2
Hf	4	6	3	4	5	4	3
Ho	1.18	0.8	0.87	0.91	2	1	1.65
In	<0.2	<0.2	<0.2	<0.2	<0.2	<0.2	<0.2
La	22.6	57.5	36.3	16.7	16.1	27.1	17.7
Lu	0.44	0.34	0.35	0.51	1.13	0.57	0.62
Mo	<2	<2	<2	<2	<2	<2	<2
Nb	18	11	14	14	24	15	39
Nd	25.8	45.9	39.2	15.7	21.2	24.5	30.2
Pb	29	12	18	16	21	18	<5
Pr	6.06	11.4	8.93	3.88	4.81	6.12	6.26
Rb	156	68.7	117	115	204	163	20.5
Sb	<0.1	<0.1	<0.1	<0.1	<0.1	0.3	0.2
Sm	6	7.4	7.8	2.9	6.3	4.7	7.9
Sn	2	<1	<1	1	3	2	3
Ta	1.3	0.5	0.8	0.8	2.7	1.5	1.8
Tb	0.95	0.71	0.83	0.56	1.42	0.7	1.33
Th	8.9	7.4	11.7	9.2	16	12.3	1.9
Tl	0.7	<0.5	<0.5	0.5	1	0.8	<0.5
Tm	0.49	0.32	0.32	0.45	1.01	0.54	0.59
U	1.91	1.05	1.7	1.13	3.8	2.42	0.37
W	<1	<1	<1	<1	<1	<1	<1
Y	34.1	21.5	25	29.5	68	29.7	40.3
Yb	3.5	2.1	2.2	3.1	7.4	3.8	3.7
Zr	174	258	97.7	133	126	129	101

Structural Geology

Ductile Structures

The rocks of the Uxbridge quadrangle occur in the core of the Milford antiform. At least four generations of ductile deformation and associated structures are recognized, and they are designated by their relative ages as D_1 to D_4 . In the following discussion, we present the ductile structures in order of their relative ages, from oldest to youngest.

Relict Deformation (D_1)

The oldest foliation is a relict layer-parallel schistosity (S_1) observed in rocks of the Blackstone Group. The relict S_1 foliation is found parallel to bedding in tight to isoclinal F_2 folds (fig. 9). The relict foliation is characterized by a

lepidoblastic texture of aligned mica, quartz, and amphibole. Definitive F_1 folds associated with this oldest foliation were not observed in this quadrangle. This relict foliation is reported to be a deformational and metamorphic fabric that predates the intrusion of the plutonic rocks in the Avalon zone, indicating that it is Neoproterozoic (Bailey and others, 1989; Goldsmith, 1991c). In the Uxbridge quadrangle, this relict S_1 foliation predates the migmatitic rocks around the small plutons of the Ironstone quartz diorite (fig. 9C), showing that the foliation is, in places, related to a Neoproterozoic metamorphic and deformational event. The plutonic rocks locally contain a deformed foliation that predates the dominant S_2 foliation in the rocks. This rare, older foliation appears along and parallel to the contacts between rocks of the Ponaganset Gneiss and Northbridge Granite Gneiss, and parallel to rare compositional banding in these rocks. It represents either an igneous flow foliation or relict metamorphic foliation.

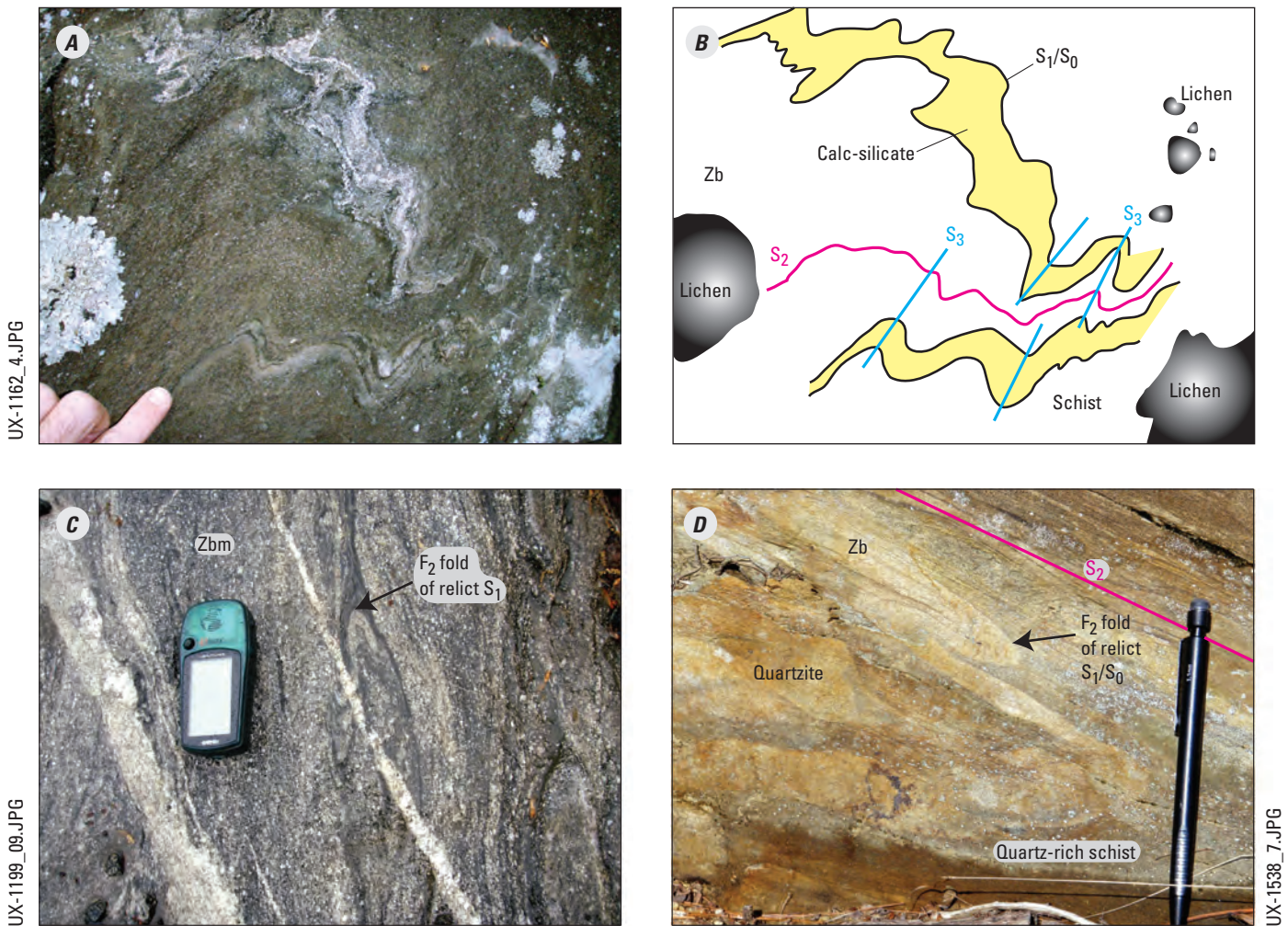


Figure 9. Photographs and sketch of relict S_1 foliation and F_2 folds in rocks of the Blackstone Group. *A*, Folded amphibole-bearing calc-silicate layers define deformed compositional layering (S_0) that is parallel to the relict S_1 foliation in the biotite schist in unit Zb. The composite S_1/S_0 foliation is deformed into an F_2 fold with the dominant foliation (S_2) marking the axial surface. Steeply dipping upright cleavage (S_3) deforms the older foliations. *B*, Sketch of *A*. *C*, Rootless isoclinal F_2 fold in the plane of the dominant foliation S_2 , showing deformed relict S_1 foliation in the migmatitic gneiss (Zbm). Light-colored granitic dikes cut the dominant foliation. GPS receiver is 10.5 cm long. *D*, Isoclinal F_2 fold of relict S_1/S_0 in the plane of the dominant foliation S_2 , showing deformed relict S_1 foliation in the Blackstone Group (Zb).

Second Generation Deformation (D_2)

The second generation foliation (S_2) is the dominant planar fabric in the Uxbridge quadrangle. The S_2 foliation is a schistosity in the Blackstone Group rocks and a gneissosity to nonpenetrative foliation in the plutonic rocks. The S_2 foliation is axial planar to tight to isoclinal folds of relict S_1 foliation in the metasedimentary Blackstone Group rocks (fig. 9D), and is axial planar to rare folds of igneous flow foliation in the intrusive rocks. Generally, the S_2 foliation in the plutonic rocks is more penetrative to the north and less penetrative to the south. This observation supports Goldsmith's (1991c) claim that the intensity of the foliation increases as the Bloody Bluff fault (fig. A on map) is approached. In areas where S_2 is a less-penetrative planar fabric, the foliation is weakly developed and locally anastomoses through the rock. In these places, the plutonic rocks generally possess an L-tectonite fabric (fig. 5) having a pronounced northeast-trending L_2 lineation

(fig. 10A). Locally the S_2 fabric is mylonitic, and in these places thin mylonite zones range from several centimeters (fig. 11) to several meters thick. S_2 is deformed into a north- to northwest- or west-striking and gently east- to northeast-dipping orientation across the quadrangle, and the poles to the foliation define a great circle corresponding to deformation across the Milford antiform (fig. 10A). Second-generation mineral lineations (L_2) form "aggregate lineations" and "grain lineations" (Piazolo and Passchier, 2002; Passchier and Trouw, 2005). The mineral lineations consist of quartz rods, and aligned biotite, hornblende, and recrystallized garnet, and deformed and recrystallized feldspar tails around microcline augen consistent with formation during upper greenschist- to lower amphibolite-facies metamorphic conditions. The L_2 mineral lineations show a very consistent northeast trend, subparallel to the F_2 fold axes or intersection lineations, suggesting high strain during D_2 deformation (fig. 10A).

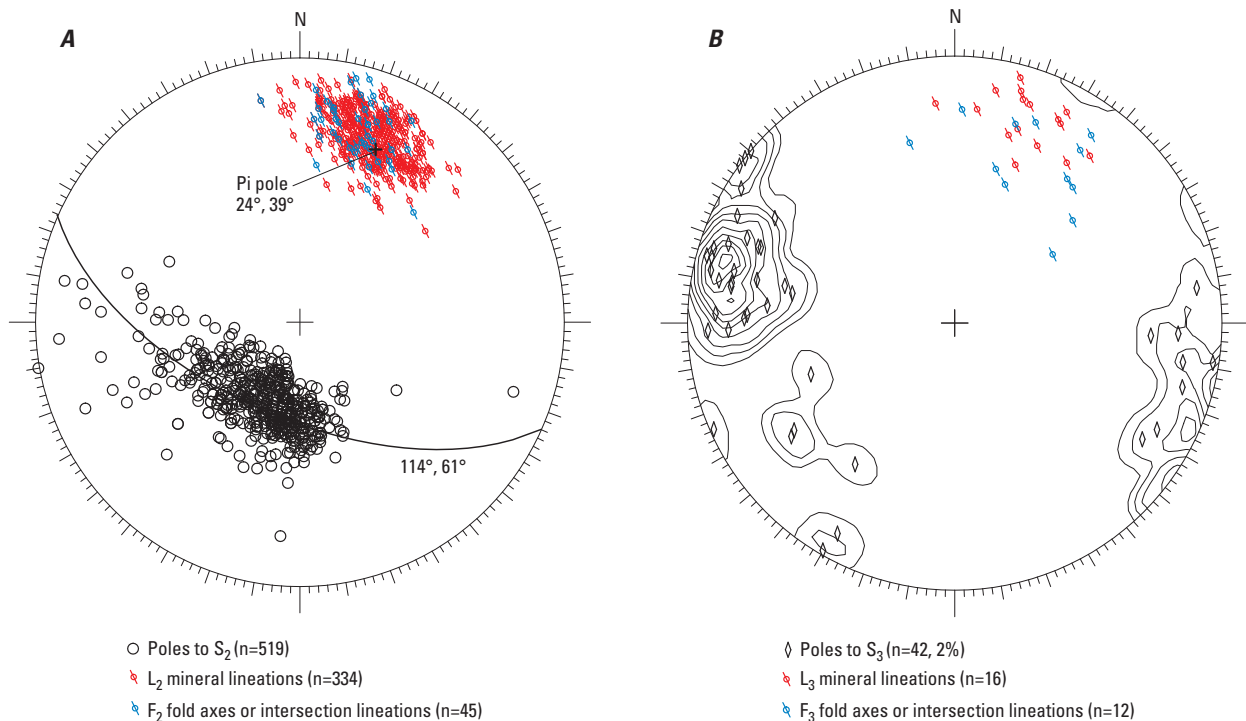


Figure 10. Summary diagrams of D_2 and D_3 ductile structures. *A*, Lower hemisphere equal-area projection (stereonet) of dominant foliation (S_2) showing the poles to S_2 , best-fit great circle to poles, the Pi pole to a best-fit great circle, L_2 mineral lineations, and F_2 fold axes. *B*, Stereonet of poles to S_3 including F_3 axial surfaces, F_3 fold axes and intersection lineations, and L_3 mineral lineations. The number of points and the contour interval (where plotted) are shown in parentheses at the bottom of each diagram. Diagrams were plotted using the Structural Data Integrated System Analyzer (DAISY) software by Salvini (2010).

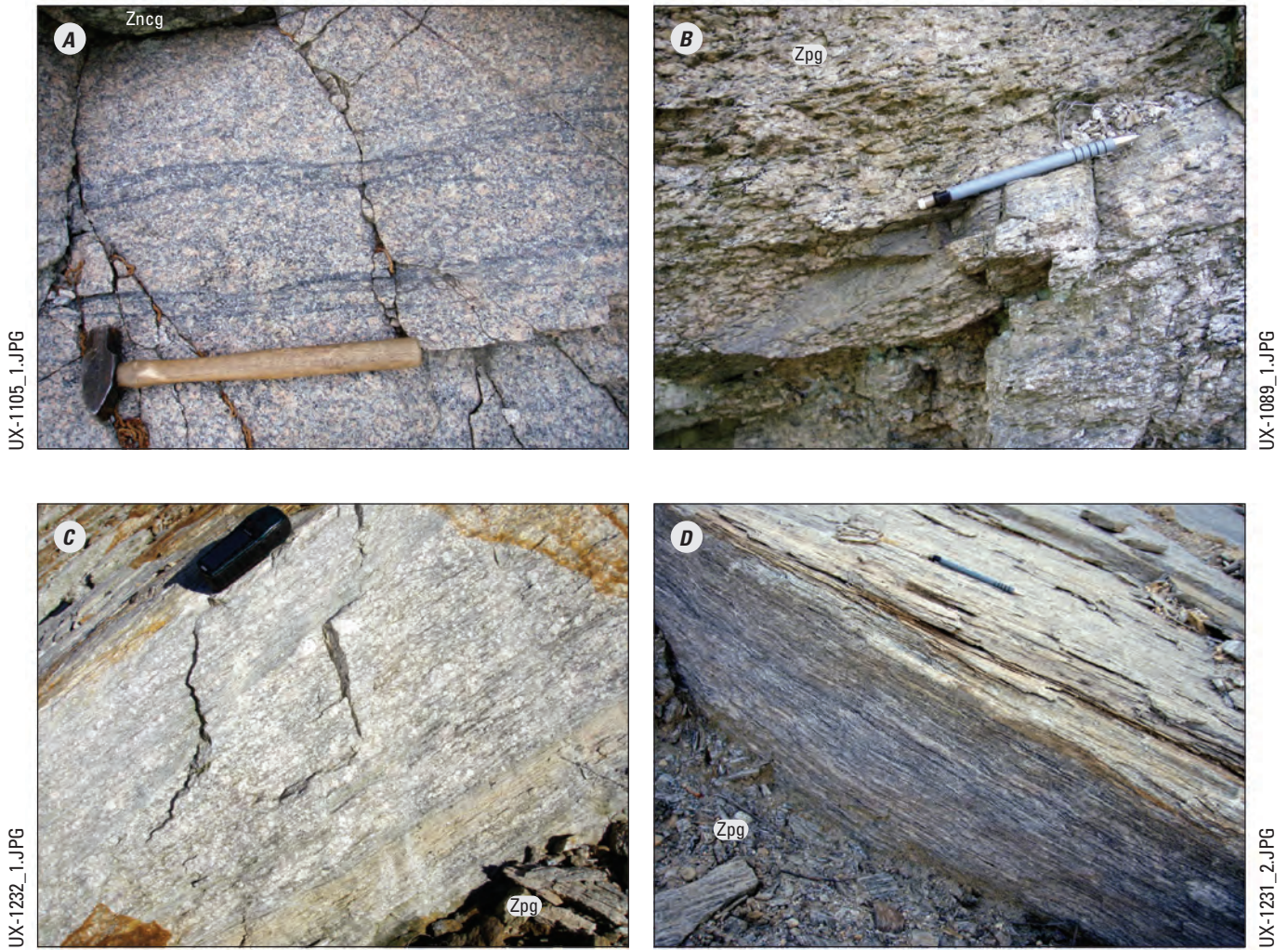


Figure 11. Photographs showing variation in the S_2 foliation in granitic rocks. *A*, Weakly developed nonpenetrative S_2 foliation is defined by darker bands of aligned biotite and recrystallized quartz and feldspar in the Northbridge Granite Gneiss (Zncg). *B*, Moderately well-developed S_2 foliation with a thin mylonite zone (under pencil) in the Ponaganset Gneiss (Zpg). *C*, Well-developed S_2 foliation with thin anastomosing mylonite zones in the Ponaganset Gneiss. GPS receiver is 10.5 cm long. *D*, Penetrative mylonitic S_2 foliation in the Ponaganset Gneiss.

Third Generation Deformation (D_3)

The third generation of ductile deformation produced the Milford antiform and open to tight folds (F_3) of the dominant foliation (S_2) (figs. 9A, 10). The F_3 folds are associated with a crenulation cleavage in the fine-grained rocks of the Blackstone Group (figs. 9A, 10). In the coarser grained rocks, such as the granitoids and quartzites, the cleavage is very weakly developed or not recognized, and the D_3 fabric is expressed as thin mylonite zones, shear bands, or kink bands (fig. 12). In the granitic rocks of the Milford antiform, outcrop-scale F_3 folds or S_3 cleavage were rarely observed. Across the quadrangle, the folding of the dominant S_2 foliation defines

the northeast-plunging Milford antiform as a major map-scale D_3 structure. The trend of F_3 fold axes and L_3 intersection lineations plunge to the north-northeast (fig. 10B). The strike and dip of S_3 is somewhat variable, but the general strike is northeast with a steep dip, although some axial surfaces and shear bands strike northwest with a northeast dip (fig. 10B). The northwest direction is at a high angle to the northeast trend of the Milford antiform, but matches the trend of the Oxford anticline (Goldsmith, 1991c; Barosh, 2005) (fig. 1A on map). The northwest trend was also observed in the Grafton quadrangle to the north, but to a lesser extent (Walsh and others, 2011).

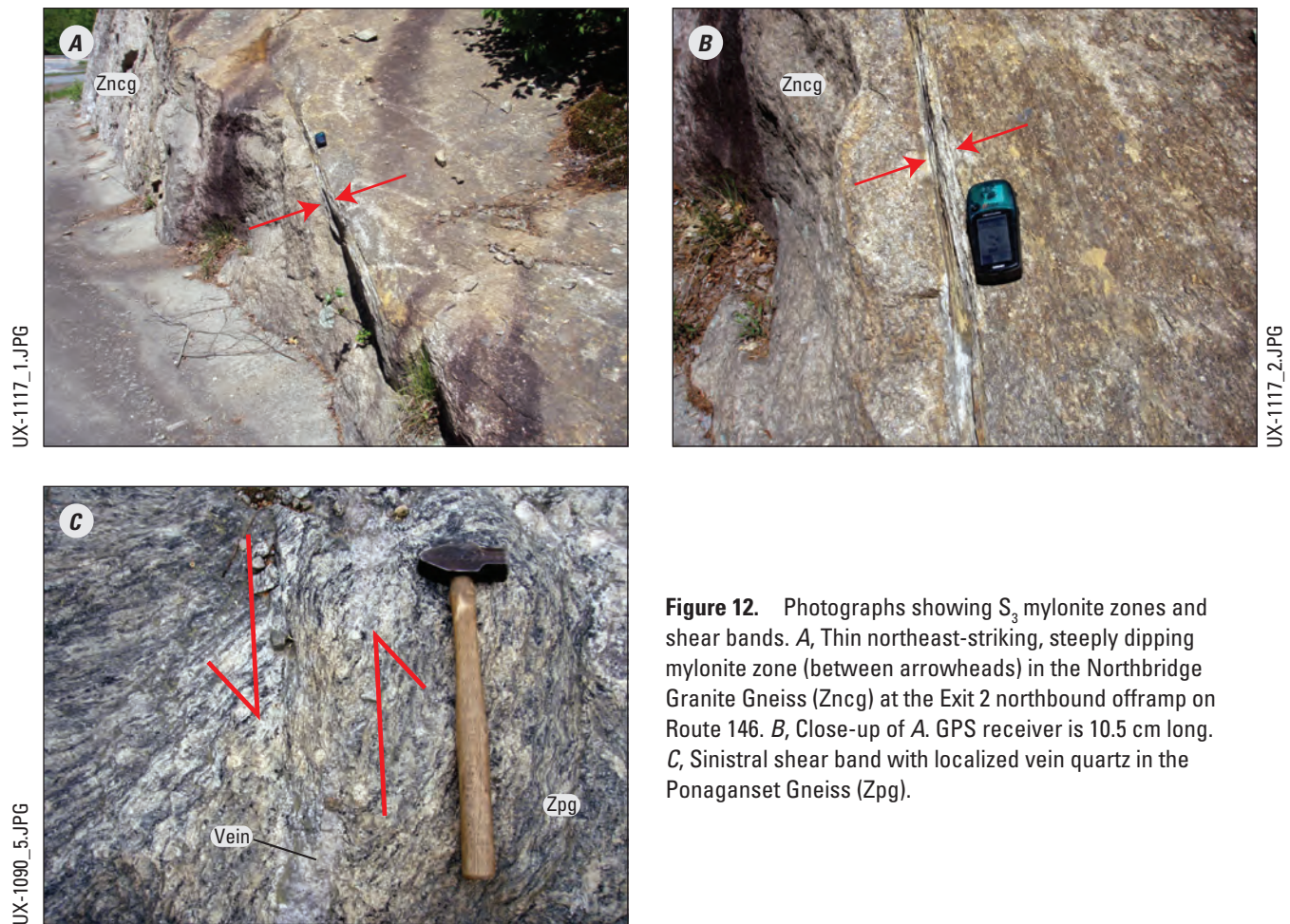


Figure 12. Photographs showing S_3 mylonite zones and shear bands. *A*, Thin northeast-striking, steeply dipping mylonite zone (between arrowheads) in the Northbridge Granite Gneiss (Zncg) at the Exit 2 northbound offramp on Route 146. *B*, Close-up of *A*. GPS receiver is 10.5 cm long. *C*, Sinistral shear band with localized vein quartz in the Ponaganset Gneiss (Zpg).

L_3 mineral lineations occur as aggregate lineations defined by aligned and recrystallized biotite, quartz, and feldspar in the plane of thin subvertical D_3 mylonite zones and shear bands. In the Grafton quadrangle to the north, aligned hornblende locally defines an L_3 mineral lineation, but in the Uxbridge quadrangle this was not observed. Instead, hornblende occurs both as aligned grains parallel to L_2 and as randomly oriented post- D_2 fascicular overgrowths in the plane of S_2 (fig. 13).

Map- and outcrop-scale S_3 mylonite zones are most abundant in the southeastern part of the quadrangle, and in this area three mylonitic faults are shown on the map. Asymmetric quartz ribbons, s-c fabrics, and oblique foliation or c-type shear bands (Passchier and Trouw, 2005, p. 128) from a sample (station 1121) in the vicinity of Exit 2² on Route 146 show sinistral, west-side-up displacement. The mapped fault east of Exit 2 was drawn based on the apparent truncation of a small belt of alaskite (Zhv) seen along the southbound onramp of Route 146. It should be noted that only a single sample was collected for kinematics from the Exit 2 area, and outcrops in the area contain multiple thin S_3 mylonite zones whose kinematics have not been studied in detail. A second S_3 mylonitic fault is mapped near the junction of Chestnut and Aldrich Streets based on the presence of steeply dipping northeast-striking mylonitic fabric exposed at two places (stations 1077 and 1078) on Acorn Drive (street name not on base map). A third fault is mapped near Aldrich Pond where S_3 mylonitic fabric with foliation-parallel quartz veins deforms the older S_2 foliation into a map-scale dextral shear band. A sample (station 1574) collected just south of the gas pipeline north of Aldrich Pond yielded no conclusive kinematic indicators, and the offset along this fault is interpreted from the mapped deflection of the S_2 foliation west of the fault.

²The location of Route 146 is not precisely depicted on the topographic base map. The latest revision to the base map occurred in 1979, and the highway is shown as a single line. Currently the highway is divided into northbound and southbound lanes. The line on the map generally shows the location of the two northbound lanes, and the two southbound lanes are not shown. Modifications to the interchanges also are not shown.



Figure 13. Photograph showing syntectonic and post-tectonic hornblende. On the left, hornblende (hb) is aligned parallel to L_2 (parallel to the red arrow and pencil), and to the right hornblende occurs as larger, post- D_2 , randomly oriented fascicular overgrowths in the plane of S_2 . Rock is a titanite-epidote-plagioclase-quartz-hornblende-biotite schist xenolith of the Blackstone Group (Zb) within the Northbridge Granite Gneiss (Zncgm). Section of pencil shown is about 10 cm long.

Fourth Generation Deformation (D_4)

A fourth period of deformation produced open, late folds that deform the S_3 foliation. This deformation was observed at only one place, north of Whitinsville (station 1435). In addition to the late folds, numerous quartz veins and pegmatite dikes postdate the D_3 fabric, and their orientations are summarized in figure 14. The veins and dikes represent a continuum of extensional deformation from D_3 to D_4 , as veins and dikes also occur in the plane of D_3 ductile shear bands (figs. 12C and 15A). Late, tabular, crosscutting quartz veins and pegmatite dikes are shown on the map by strike and dip symbols. In many places, the veins and dikes are zoned and show gradations from quartz veins to muscovite granite pegmatite and more rarely biotite granite pegmatite along the margins or along the median line (figs. 4 and 15C, D). Veins show a preferred northwest strike and steep northeast dip (fig. 14A) corresponding to a principal trend of $301^\circ \pm 7^\circ$ (fig. 14B), and a subordinate trend to the northeast. The pegmatite dikes show random orientations (fig. 14C).

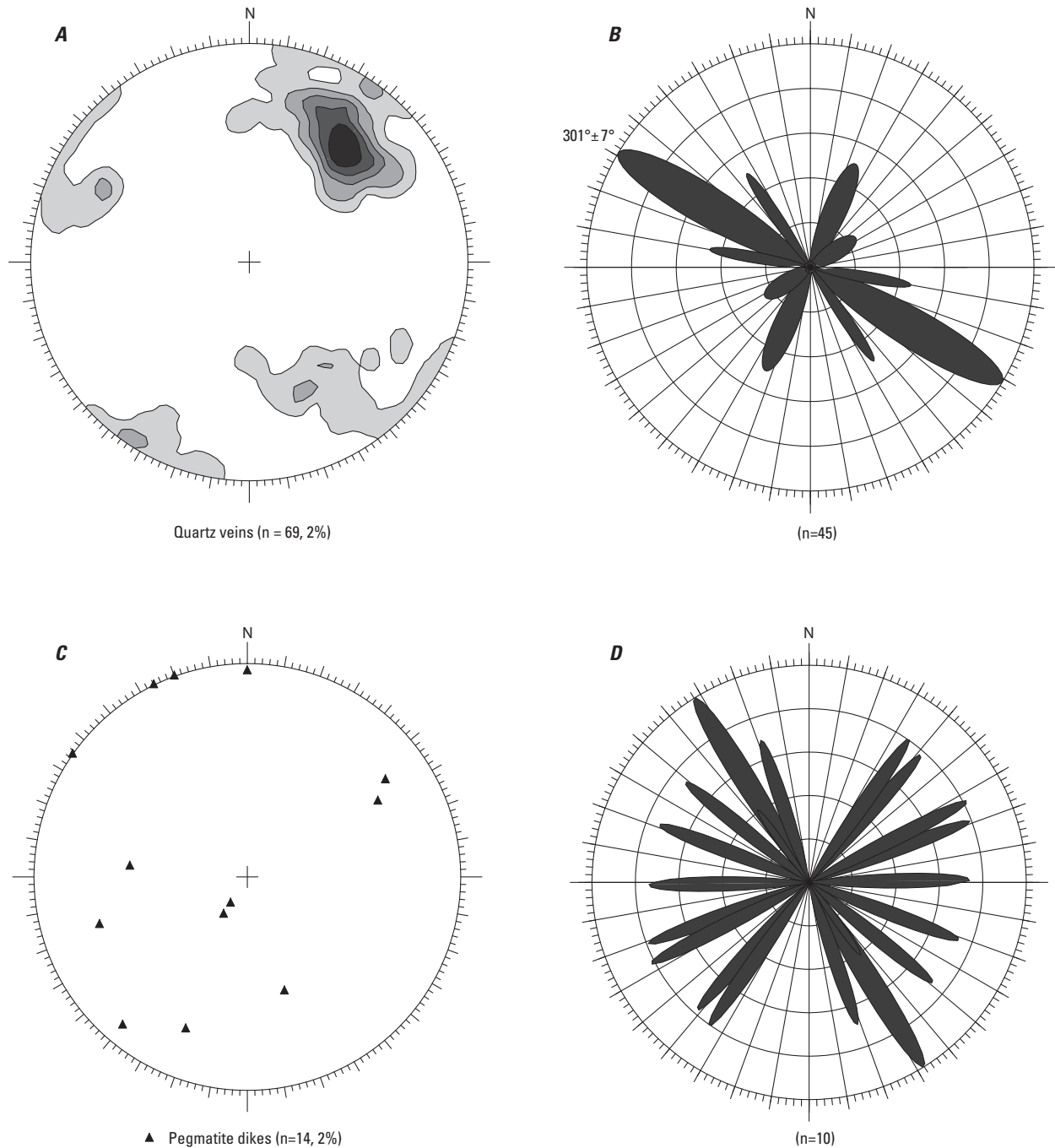


Figure 14. Summary diagrams showing the orientation of quartz veins and pegmatite dikes. *A*, Stereonet of contoured poles to strike and dip of veins. *B*, Normalized azimuth-frequency (rose) diagram of steeply dipping (dips $>60^\circ$) veins. The principal trend ($301^\circ \pm 7^\circ$) is shown with one standard deviation error. *C*, Stereonet of poles to strike and dip of dikes. *D*, Rose diagram of steeply dipping (dips $>60^\circ$) dikes. For all diagrams, the number of points and the contour interval (where plotted) are shown in parentheses at the bottom of each diagram. Diagrams were plotted using the Structural Data Integrated System Analyzer (DAISY) software by Salvini (2010).

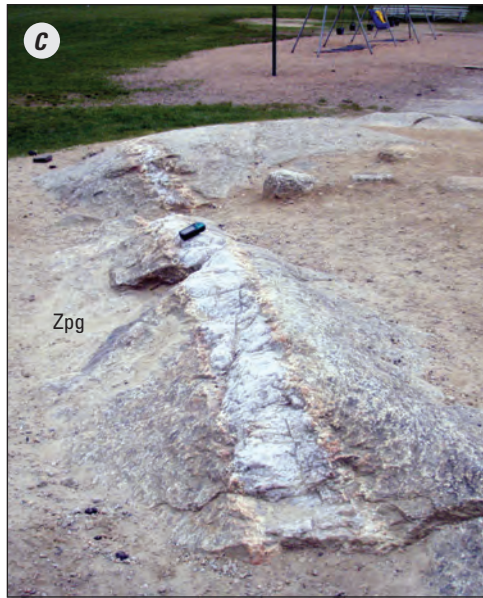


UX-1090_7.JPG

Figure 15. Photographs of quartz veins and pegmatite dikes. *A*, Quartz vein in a shear band showing marginal granitic pegmatite within the Ponaganset Gneiss (Zphg). *B*, Multiple quartz veins at Reservoir No. 5 in Sutton. *C*, Tabular, approximately 30-cm-thick vein with a pegmatitic margin exposed at the Douglas Elementary School. *D*, Zoned granitic pegmatite dike in the Northbridge Granite Gneiss (Zncgm). The center of the dike contains coarse biotite and pale-green-weathering plagioclase. GPS receiver in *C* and *D* is 10.5 cm long.



UX-1054_4.JPG



UX-1104_2.JPG



UX-1281_3.JPG

Comment on the Hope Valley Shear Zone

An Alleghanian fault called the Hope Valley shear zone (HVsz) has been interpreted to pass through the Uxbridge quadrangle and represent a regionally significant terrane boundary between the Hope Valley terrane to the west and the Esmond-Dedham terrane to the east (O'Hara and Gromet, 1985). The northern part of the shear zone is supposed to be at the contact between the Hope Valley Alaskite Gneiss and the Ponaganset Gneiss in the Grafton quadrangle (O'Hara and Gromet, 1985; Gromet and O'Hara, 1985; Hermes and others, 1994). Mylonitic foliation found in the Ponaganset Gneiss on Route 146 in the town of Sutton in the Grafton quadrangle (Walsh and others, 2011) was attributed to southward thrusting at a high angle to the overall right-lateral offset along the Hope Valley shear zone (O'Hara and Gromet, 1985; Gromet and O'Hara, 1985). Wayne and others (1992) obtained conventional U-Pb ages of 285 ± 25 and 270 ± 92 Ma from metamorphic zircons in a mylonite at this location, indicating Alleghanian deformation and metamorphism of the Neoproterozoic plutonic rocks. Gromet and O'Hara (1985) noted correctly that the mylonites and foliation at the roadcut in the Grafton quadrangle strike at a right angle to the inferred trend of the HVsz, but Wayne and others (1992) incorrectly stated that the mylonites had a north-south strike and dipped gently to the west parallel to the HVsz.

Mapping in the Grafton and Uxbridge quadrangles does not support the existence of the Hope Valley shear zone for the following reasons:

- Numerous thin (<10-cm-thick) mylonite zones are visible at the Route 146 roadcut in the Grafton quadrangle (and at many other roadcuts), but no single zone appears to be more significant than the other. Each thin mylonite zone represents internal deformation parallel to the dominant foliation within the Ponaganset Gneiss.
- The Hope Valley Alaskite Gneiss intrudes both the Ponaganset Gneiss and the Northbridge Granite Gneiss, and there is no distinct mylonitic fabric between the Hope Valley Alaskite Gneiss and the Ponaganset Gneiss.
- In the Grafton quadrangle, there is no fabric in the rock that strikes north-south and dips subvertically, parallel to the proposed HVsz. The dominant foliation and the thin mylonite zones near the proposed location of the HVsz strike east-west and dip gently north. Thus, the dominant foliation is virtually at a right angle to the proposed location of the shear zone (recognized by Gromet and O'Hara, 1985). In the Uxbridge quadrangle, the north-south-striking, steeply dipping shear zones and thin mylonites are related to D_3 deformation and represent internal deformation within the Ponaganset Gneiss and Northbridge Granite Gneiss, but these shear zones do not continue north into the Grafton quadrangle.
- O'Hara and Gromet (1985) and Gromet and O'Hara (1985) stated that considerable differences existed between the rocks of the Hope Valley and Esmond-Dedham terranes on either side of the HVsz. This may be true in Rhode Island at the type locality, but in contrast, geochemical and geochronologic data (this study and Walsh and others, 2011) for the Hope Valley Alaskite Gneiss and Northbridge Granite Gneiss are quite similar and demonstrate that these rocks, located on either side of the proposed HVsz, cannot be separated into two terranes on a geochemical or age basis. Chemical data from the Grafton and Uxbridge quadrangles support work by Wones and Goldsmith (1991), suggesting that the Hope Valley and Northbridge (formerly Scituate) are similar.

Brittle Structures

The planar brittle structures in this study are also called fractures. Fractures with slickensides or visible displacement are brittle faults. Fractures without visible displacement are separated based on whether or not they are related to an older fabric in the metamorphic and igneous rocks, as follows:

- Parting fractures occur where the rocks break, or part, along a pre-existing fabric. Parting fractures are related to older sedimentary, igneous, or metamorphic fabrics due to structural inheritance and occur along dikes, veins, axial surfaces of folds, shear bands, cleavage, and foliation.
- Fractures that cross the metamorphic or igneous fabric of the rocks include brittle faults, joints, and joint sets.

The orientation of measured joints includes those with trace lengths greater than 20 cm (Barton and others, 1993). Joints were measured subjectively using methods described in Spencer and Kozak (1976) and Walsh and Clark (2000), and the database includes only the most conspicuous joints observed in a given outcrop. Fracture data (fig. 16) are plotted on azimuth-frequency or rose diagrams and stereonet (lower hemisphere equal-area projections) using Structural Data Integrated System Analyzer (DAISY) software (Salvini, 2010). The software generates rose diagrams using a Gaussian curve-fitting routine for determining peaks in directional data (Salvini and others, 1999) that was first described by Wise and others (1985). The rose diagrams include strike data for steeply dipping fractures (dips $\geq 60^\circ$, after Mabee and others, 1994).

Fracture data are summarized in figure 16 and the original data are located in the GIS database. In general, the most conspicuous fractures occur in three categories (fig. 17): (1) parting fractures parallel to the dominant foliation (called “foliation-parallel fractures” by Manda and others, 2008), (2) steeply dipping fractures that cross the foliation at a high angle, and (3) steeply dipping fractures that are orthogonal to the foliation. In the northwestern part of the quadrangle where there is extensive outcrop, pronounced topographic features (lineaments) are controlled by these three fracture types. Gently dipping sheeting fractures are not widespread in this quadrangle because most of the gently dipping fractures are parting fractures that occur parallel to the dominant S_2 foliation (fig. 16A). Steeply dipping joints are dominated by either abutting or throughgoing fractures that cross entire outcrops with trace lengths on the order of meters (fig. 17). Throughgoing joints tend to cross the foliation at a high angle, and these joints are called “crossing” fractures (Barton and others, 1993). These steeply dipping crossing fractures show preferred northeast trends (19° – 34° , fig. 16). The northeast

trend of steeply dipping crossing fractures is similar to the trend of some planar pegmatite dikes, the trend of the dominant mineral lineation, and the trend of the Milford antiform, suggesting that brittle failure was inherited and occurred not only along igneous planar features but also along ductile linear features in the rock. The steeply dipping, generally northwest-southeast to east-west trend represents joints that are orthogonal to the dominant foliation (fig. 17).

The spacing of fractures, although not quantified in this study, rarely exceeds a few meters. Spacing of steeply dipping, crossing and orthogonal joints in igneous rocks locally exceeds several meters. The spacing and abundance of foliation-parallel fractures, or parting fractures, is related to rock type: finer grained rocks exhibit more parting fractures and smaller spacing. Joint data, separated by generalized rock type (fig. 16D–G), show that the metasedimentary and igneous rocks have overall similar joint trends, with northeast-trending joints showing more prominence in the igneous rocks than in the metasedimentary rocks. Parting by rock type is shown in table 6. Generally, the Northbridge Granite Gneiss exhibits less parting than the Ponaganset Gneiss, while the Blackstone Group metasedimentary rocks exhibit the most parting, although overall the degree of parting is quite similar.

Table 6. Summary of foliation-parallel parting fractures by formation and rock type.

Formation or rock type	Number of measurements that exhibit parting fractures along the foliation	Total number of foliation measurements	Parting fractures as a percentage of total foliation measurements
Formation			
Hope Valley Alaskite Gneiss	5	6	83
Tonalite and granodiorite gneiss	10	15	67
Blackstone Group	53	92	58
Ponaganset Gneiss	136	244	56
Northbridge Granite Gneiss	100	204	49
Rock type			
Metasedimentary rocks	53	92	58
Igneous rocks	251	469	54

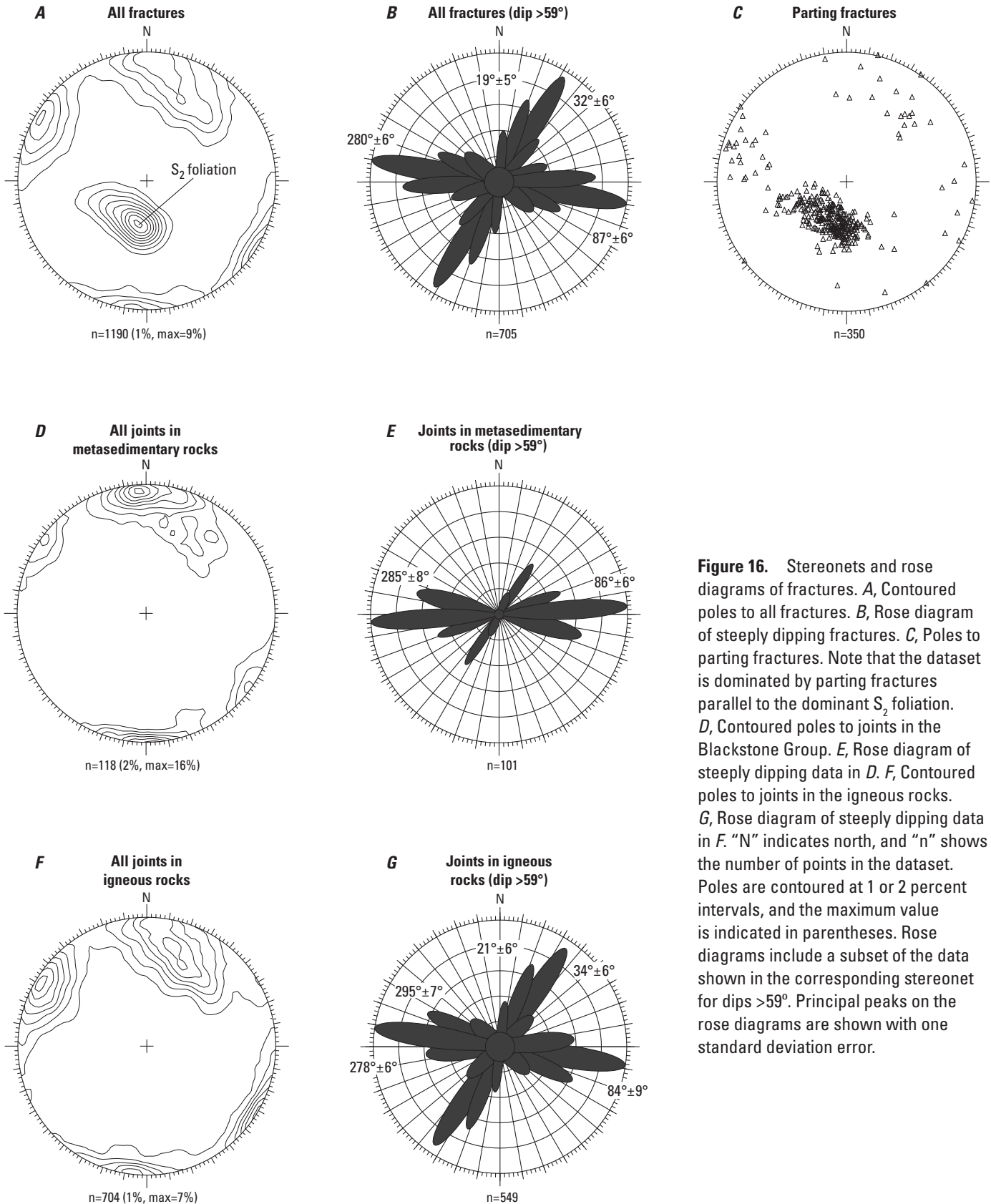


Figure 16. Stereonets and rose diagrams of fractures. *A*, Contoured poles to all fractures. *B*, Rose diagram of steeply dipping fractures. *C*, Poles to parting fractures. Note that the dataset is dominated by parting fractures parallel to the dominant S_2 foliation. *D*, Contoured poles to joints in the Blackstone Group. *E*, Rose diagram of steeply dipping data in *D*. *F*, Contoured poles to joints in the igneous rocks. *G*, Rose diagram of steeply dipping data in *F*. “N” indicates north, and “n” shows the number of points in the dataset. Poles are contoured at 1 or 2 percent intervals, and the maximum value is indicated in parentheses. Rose diagrams include a subset of the data shown in the corresponding stereonet for dips >59°. Principal peaks on the rose diagrams are shown with one standard deviation error.

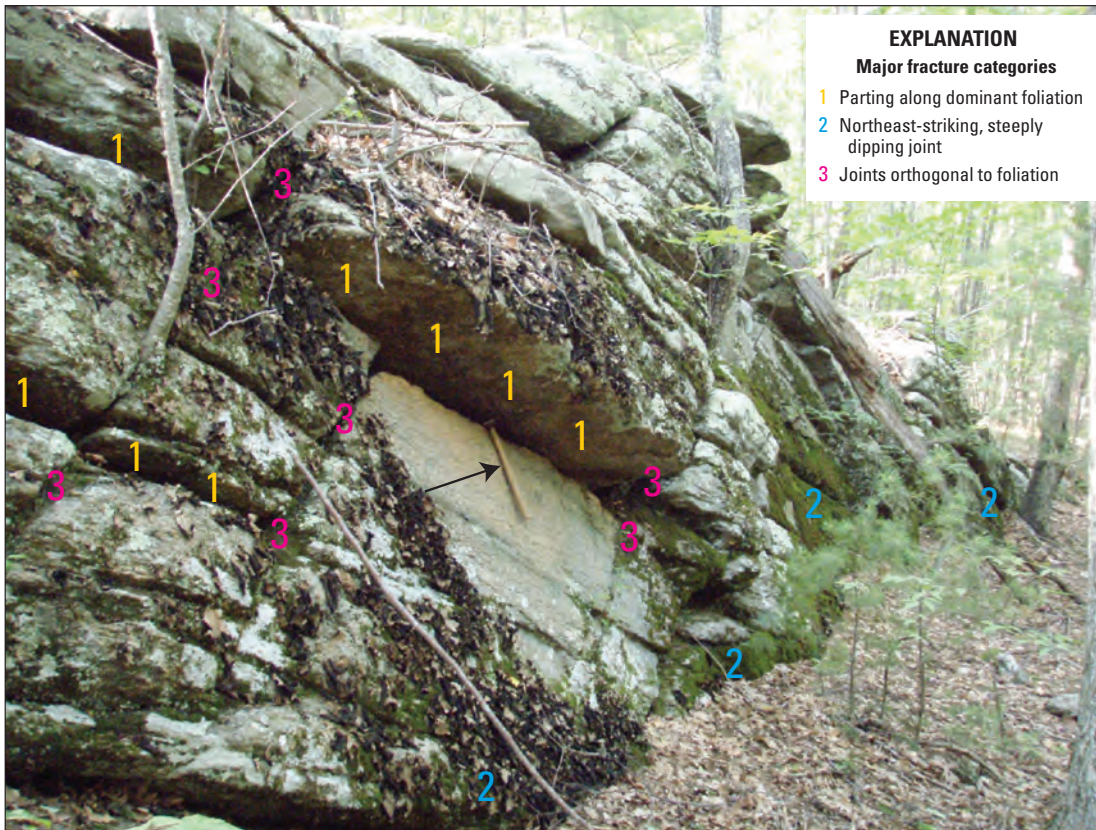


Figure 17. Photograph showing three main categories of fractures. Parting fractures (1) occur along the dominant foliation and create the overhanging block in this photograph. The main cliff face (2) is a northeast-striking throughgoing joint. Joints that are orthogonal to the foliation (3) are both throughgoing and abutting in this example. Outcrop is Ponaganset Gneiss. Hammer for scale (arrow).

Brittle Faults

Five outcrop-scale brittle faults were identified by slickensides or Riedel shears, and they are shown on the map with strike and dip symbols and their associated bearing and plunge of linear slickenlines. The faults show normal (1), reverse (2), and left-lateral (3) strike-slip motion. The orientations are variable and the small number of faults prevents a comprehensive analysis. Assuming, however, that the faults are coeval, a calculation of the mean P and T axes (Angelier, 1979) (fig. 18) shows a calculated average stress field that is consistent with Late Triassic to Early Jurassic northwest-southeast extension associated with rifting of the New England crust during the initial opening of the Atlantic basin (Kaye, 1983; de Boer and Clifford, 1988; Manning and de Boer, 1989; Goldsmith, 1991c). The limited brittle fault data in Uxbridge agree with findings in the Grafton quadrangle to the north (Walsh and others, 2011).

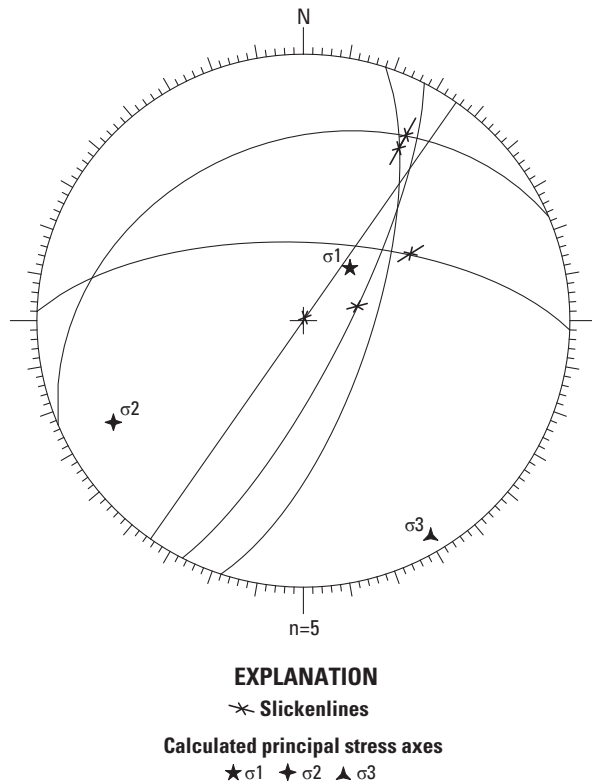


Figure 18. Stereonet showing results of brittle fault inversion analysis. Projection shows fault planes, slickenlines, and calculated stress tensors including the mean P and T axes for five brittle faults (n =number of faults). Shortening (P) axis= σ_1 , and extension (T) axis= σ_3 . Inversion analysis was calculated using the Structural Data Integrated System Analyzer (DAISY) software by Salvini (2010).

Metamorphism

The Avalon zone makes up the lower-plate rocks on the south side of the Bloody Bluff fault. These rocks experienced a different metamorphic history than the Nashoba zone rocks of the upper plate to the north and west (Wintsch and Aleinikoff, 1987; Goldsmith, 1991c). In the area of the Milford antiform, the upper-plate rocks in the Nashoba zone experienced upper amphibolite-facies metamorphic conditions, whereas the rocks in the lower-plate Avalon zone experienced upper greenschist- to lower amphibolite-facies metamorphic conditions. The timing of peak metamorphism in the Nashoba zone is considered to be early Paleozoic (Goldsmith, 1991c; Wintsch and others, 1991, 1992, 1993, 2007; Hepburn and others, 1995; Stroud and others, 2009). In contrast to the Nashoba zone, early metamorphism in the Avalon zone is considered to be Neoproterozoic (Goldsmith, 1991c; Hepburn and Bailey, 1998; Attenoukon and others, 2005; Attenoukon, 2008), and peak metamorphism is considered to be late Paleozoic, related to Alleghanian orogenesis (Wintsch and Sutter, 1986; Wintsch and Aleinikoff, 1987; Zartman and others, 1988; Gromet, 1989; Getty and Gromet, 1992a,b; Wintsch and others, 1991, 1992, 1993, 1998, 2007; Gromet and others, 1998; Walsh and others, 2007; Attenoukon, 2008).

The timing of Neoproterozoic metamorphism in relation to the earliest episode of deformation (D_1) is not well constrained. Goldsmith (1991c) reported that the metamorphism predated the Neoproterozoic plutonic events, and that metamorphism may have been related to subduction. Hepburn and Bailey (1998) attributed the early thermal event to contact metamorphism. In this map area, migmatization adjacent to the Ironstone quartz diorite of Emerson (1917) provides solid evidence for Neoproterozoic contact metamorphism, and shows that it postdates a relict metamorphic fabric in the Blackstone Group rocks. In the Grafton quadrangle to the north (Walsh and others, 2011) the early D_1 fabric is locally observed as aligned tremolite in the Westboro Formation. Attenoukon (2008) reported a $^{40}\text{Ar}/^{39}\text{Ar}$ amphibole cooling age of 588 Ma from a gabbro in the Holliston quadrangle in the northeastern part of the Milford antiform, providing firm evidence for a Neoproterozoic thermal event.

The dominant metamorphic event produced the penetrative gneissic fabric (S_2) in the rocks of the Milford antiform. The timing of D_2 deformation in the Milford antiform is constrained by the age of syn- D_2 mylonites dated in the Grafton quadrangle and by syntectonic development of L_2 hornblende lineations and lower amphibolite-facies mineral assemblages in S_2 . Wayne and others (1992) report conventional U-Pb metamorphic zircon ages of 285 ± 25 and 270 ± 92 Ma from mylonitic rocks exposed in the Grafton quadrangle on Route 146 in the Ponaganset Gneiss; these mylonites developed during D_2 . $^{40}\text{Ar}/^{39}\text{Ar}$ amphibole and

biotite cooling ages in the Milford antiform range from 268 to 250 Ma, and K-feldspar cooling ages range from 254 to 227 Ma (Attenoukon and others, 2005; Attenoukon, 2008). Within the Avalon zone, Attenoukon (2008) documented an Alleghanian metamorphic gradient that increases to the west and is truncated by the Bloody Bluff fault. The rocks in the Uxbridge quadrangle are within the area affected by peak Alleghanian amphibolite-facies metamorphism. Thus, peak Alleghanian metamorphism probably occurred during the late Carboniferous to early Permian, followed by continuous cooling associated with uplift. Randomly oriented hornblende porphyroblasts in the plane of S_2 (fig. 13), found here and in the Grafton quadrangle, indicate that Alleghanian hornblende crystal growth continued after D_2 . D_3 fabrics include formation of the Milford antiform and associated shear bands and thin mylonite zones developed during the waning stage of Alleghanian deformation and metamorphism. The late D_4 intrusion of tabular pegmatites and quartz veins marks the final extensional stage of deformation during upper greenschist- to lower amphibolite-facies metamorphism.

Economic Geology

The locations of 16 abandoned granite quarries and 1 abandoned silver mine were confirmed during mapping in the Uxbridge quadrangle, and are shown on the map and in the GIS database. Dale (1923) provides a detailed description

of the Blanchard quarries on Quarry Hill in Uxbridge, and this area represents the largest granite quarrying operation in this quadrangle. The Blanchard quarries opened in 1864 (Dale, 1923) and were known for producing some of the finest granites in Worcester County (Crane, 1907). The rock is locally referred to as the “Blanchard granite” (Rowcroft and Doherty, 2007). The map and GIS database show one quarry symbol on Quarry Hill, but the area in fact contains a number of closely spaced water-filled quarries that are shown as small ponds on the map (see also fig. 2E). The abandoned Scadden Silver Mine is located on the property of the Blissful Meadows Golf Club on Chockalogue Road in Uxbridge. Jackson (1840, p. 74) reported the presence of galena, sphalerite, and pyrite in a quartz-feldspar vein, but greatly overestimated the amount of silver in the ore at 7.110 pounds per ton. Nearby outcrops consist of Blackstone Group quartzite. The failed mine was briefly operational around 1837 according to a sign posted at the golf course (fig. 19) and the course’s Web site,³ which cites an article from a former local newspaper, the Uxbridge Compendium, dated May 28, 1886. The location of the silver mine is inaccurately shown on the U.S. Geological Survey (USGS) Mineral Resources Data System,⁴ about 2.8 km to the east-northeast of the actual site, probably because it was derived from a 1:500,000-scale map (Pearre, 1956). The site is shown as a lead-zinc occurrence by Pearre (1956).

³<http://www.blissfulmeadows.com/>

⁴<http://tin.er.usgs.gov/mrds/>



Figure 19. Photographs of the abandoned Scadden Silver Mine. *A*, Outcrop of quartzite to the left shows a pronounced L_2 intersection lineation (parallel to arrow) plunging to the northeast. Mine tailings (center) are located next to the gated mine shaft (right). *B*, Sign posted on the gate.

Acknowledgments

This report was improved by the thoughtful, constructive comments of Daniel P. Murray of the University of Rhode Island and Arthur J. Merschat of the USGS.

References Cited

- Angelier, Jacques, 1979, Determination of the mean principal directions of stresses for a given fault population: *Tectonophysics*, v. 56, no. 3–4, p. T17–T26.
- Attenoukon, M.B., 2008, Thermochronological and petrographic constraints on the timing of terrane assembly in eastern New England: Bloomington, Indiana University, unpublished Ph.D. dissertation, 300 p.
- Attenoukon, M.B., Kunk, M.J., and Wintsch, R.P., 2005, Thermochronological and petrographic constraints on the timing of terrane assembly in eastern New England [abs.]: *Geological Society of America Abstracts with Programs*, v. 37, no. 7, p. 345.
- Bailey, R.H., Skehan, J.W., Dreier, R.B., and Webster, M.J., 1989, Olistostromes of the Avalonian terrane of southeastern New England, *in* Horton, J.W., Jr., and Rast, Nicholas, eds., *Mélanges and olistostromes of the U.S. Appalachians*: Geological Society of America Special Paper 228, p. 93–112.
- Barker, F., 1979, Trondhjemite; definition, environment and hypotheses of origin, *in* Barker, F., ed., *Trondhjemites, dacites, and related rocks*: Amsterdam, The Netherlands, Elsevier, p. 1–12.
- Barosh, P.J., 2005, Bedrock geologic map of the Oxford quadrangle, Worcester County, Massachusetts, Providence County, Rhode Island, and Windham County, Connecticut: Amherst, Mass., Office of the Massachusetts State Geologist, unnumbered Open-File Report, scale 1:24,000, draft available for inspection at http://www.geo.umass.edu/stategeologist/frame_maps.htm.
- Barton, C.C., Larsen, Eric, Page, W.R., and Howard, T.M., 1993, Characterizing fractured rock for fluid-flow, geo-mechanical, and paleostress modeling; methods and preliminary results from Yucca Mountain, Nevada: U.S. Geological Survey Open-File Report 93–269, 62 p., 1 pl. in pocket.
- Crane, E.B., 1907, *Historic homes and institutions and genealogical and personal memories of Worcester County, Massachusetts, with a history of Worcester Society of Antiquity*: New York, Lewis Publishing Co., 385 p.
- Dale, T.N., 1908, The chief commercial granites of Massachusetts, New Hampshire, and Rhode Island: U.S. Geological Survey Bulletin 354, 228 p.
- Dale, T.N., 1923, The commercial granites of New England: U.S. Geological Survey Bulletin 738, 488 p.
- de Boer, J.Z., and Clifford, A.E., 1988, Mesozoic tectogenesis; development and deformation of “Newark” rift zones in the Appalachians (with special emphasis on the Hartford basin, Connecticut), *in* Manspeizer, Warren, ed., *Triassic-Jurassic rifting; continental breakup and the origin of the Atlantic Ocean and passive margins: Developments in Geotectonics* 22, pt. A, p. 275–306.
- Dixon, H.R., 1974, Bedrock geologic map of the Thompson quadrangle, Windham County, Connecticut, and Providence County, Rhode Island: U.S. Geological Survey Geologic Quadrangle Map GQ–1165, scale 1:24,000.
- Emerson, B.K., 1917, Geology of Massachusetts and Rhode Island: U.S. Geological Survey Bulletin 597, 289 p., 1 pl. in pocket, scale 1:250,000.
- Emerson, B.K., and Perry, J.H., 1907, The green schists and associated granites and porphyries of Rhode Island: U.S. Geological Survey Bulletin 311, 74 p.
- Getty, S.R., and Gromet, L.P., 1992a, Geochronological constraints on ductile deformation, crustal extension, and doming about a basement-cover boundary, New England Appalachians: *American Journal of Science*, v. 292, no. 6, p. 359–397.
- Getty, S.R., and Gromet, L.P., 1992b, Evidence for extension at the Willimantic dome, Connecticut; implications for the late Paleozoic tectonic evolution of the New England Appalachians: *American Journal of Science*, v. 292, no. 6, p. 398–420.
- Goldsmith, Richard, 1991a, Stratigraphy of the Milford-Dedham zone, eastern Massachusetts; an Avalonian terrane, *in* Hatch, N.L., Jr., ed., *The bedrock geology of Massachusetts*: U.S. Geological Survey Professional Paper 1366 E–J, p. E1–E62.
- Goldsmith, Richard, 1991b, Stratigraphy of the Nashoba zone, eastern Massachusetts; an enigmatic terrane, *in* Hatch, N.L., Jr., ed., *The bedrock geology of Massachusetts*: U.S. Geological Survey Professional Paper 1366 E–J, p. F1–F22.
- Goldsmith, Richard, 1991c, Structural and metamorphic history of eastern Massachusetts, *in* Hatch, N.L., Jr., ed., *The bedrock geology of Massachusetts*: U.S. Geological Survey Professional Paper 1366 E–J, p. H1–H63.

- Gradstein, F.M., Ogg, J.G., Smith, A.G., Agterberg, F.P., Bleeker, W., Cooper, R.A., Davydov, V., Gibbard, P., Hinnov, L.A., House, M.R., Lourens, L., Luterbacher, H.P., McArthur, J., Melchin, M.J., Robb, L.J., Shergold, J., Villeneuve, M., Wardlaw, B.R., Ali, J., Brinkhuis, H., Hilgen, F.J., Hooker, J., Howarth, R.J., Knoll, A.H., Laskar, J., Monechi, S., Plumb, K.A., Powell, J., Raffi, I., Röhl, U., Sadler, P., Sanfilippo, A., Schmitz, B., Shackleton, N.J., Shields, G.A., Strauss, H., Van Dam, J., van Kolschoten, T., Veizer, J., and Wilson, D., 2004, *A geologic time scale 2004*: Cambridge, U.K., Cambridge University Press, 589 p.
- Gromet, L.P., 1989, Avalonian terranes and late Paleozoic tectonism in southeastern New England; constraints and problems, *in* Dallmeyer, R.D., ed., *Terranes in the circum-Atlantic Paleozoic orogens*: Geological Society of America Special Paper 230, p. 193–211.
- Gromet, L.P., and O'Hara, K.D., 1985, The Hope Valley shear zone—A major late Paleozoic ductile shear zone in southeastern New England, *in* New England Intercollegiate Geological Conference, 77th Annual Meeting, New Haven, Conn., Oct. 4–6, 1985, *Guidebook for field trips in Connecticut and adjacent areas of New York and Rhode Island*: Connecticut Geological and Natural History Survey Guidebook 6, p. 277–295. (Edited by R.J. Tracy.)
- Gromet, L.P., Getty, S.R., and Whitehead, E.K., 1998, Late Paleozoic orogeny in southeastern New England; a mid-crustal view, *in* New England Intercollegiate Geological Conference, 90th Annual Meeting, Kingston, R.I., Oct. 9–11, 1998, *Guidebook to field trips in Rhode Island and adjacent regions of Connecticut and Massachusetts*: Kingston, R.I., University of Rhode Island, p. B2-1–B2-19. (Edited by D.P. Murray.)
- Hepburn, J.C., and Bailey, R.H., 1998, The Avalon and Nashoba terranes in eastern Massachusetts, *in* New England Intercollegiate Geological Conference, 90th Annual Meeting, Kingston, R.I., Oct. 9–11, 1998, *Guidebook to field trips in Rhode Island and adjacent regions of Connecticut and Massachusetts*: Kingston, R.I., University of Rhode Island, p. C3-1–C3-24. (Edited by D.P. Murray.)
- Hepburn, J.C., Dunning, G.R., and Hon, R., 1995, Geochronology and regional tectonic implications of Silurian deformation in the Nashoba terrane, southeastern New England, U.S.A., *in* Hibbard, J.P., van Staal, C.R., and Cawood, P.A., eds., *Current perspectives in the Appalachian-Caledonian orogen*: Geological Association of Canada Special Paper 41, p. 349–366.
- Hermes, O.D., and Zartman, R.E., 1992, Late Proterozoic and Silurian alkaline plutons within the southeastern New England Avalon zone: *Journal of Geology*, v. 100, no. 4, p. 477–486.
- Hermes, O.D., Gromet, L.P., and Murray, D.P., comps., 1994, *Bedrock geologic map of Rhode Island*: Kingston, R.I., University of Rhode Island, Rhode Island Map Series Map 1, scale 1:100,000.
- Hibbard, J.P., van Staal, C.R., Rankin, D.W., and Williams, H., 2006, *Lithotectonic map of the Appalachian orogen, Canada-United States of America*: Geological Survey of Canada Map 2096A, scale 1:1,500,000.
- Irvine, T.N., and Baragar, W.R.A., 1971, A guide to the chemical classification of the common volcanic rocks: *Canadian Journal of Earth Sciences*, v. 8, no. 5, p. 523–548.
- Jackson, C.T., 1840, *Report on the geological and agricultural survey of the State of Rhode Island, made under a resolve of [the] Legislature in the year 1839*: Providence, B. Cranston and Co., 312 p.
- Kaye, C.A., 1983, Discovery of a Late Triassic basin north of Boston and some implications as to post-Paleozoic tectonics in northeastern Massachusetts: *American Journal of Science*, v. 283, no. 10, p. 1060–1079.
- Kopera, J.P., and Shaw, C.E., Jr., 2008, *Preliminary bedrock geology of the northern portion of the Blackstone quadrangle, Massachusetts*: Office of the Massachusetts State Geologist, Open-File Report 08–03, scale 1:24,000.
- Kopera, J.P., Shaw, C.E., Jr., and Fernandez, Maria, 2007, *Preliminary bedrock geologic map of the Milford quadrangle, Massachusetts*: Office of the Massachusetts State Geologist, Open-File Report 07–01, 4 sheets, scales 1:24,000 and 1:72,000.
- Mabee, S.B., Hardcastle, K.C., and Wise, D.U., 1994, A method of collecting and analyzing lineaments for regional-scale fractured-bedrock aquifer studies: *Ground Water*, v. 32, no. 6, p. 884–894.
- Manda, A.K., Mabee, S.B., and Wise, D.U., 2008, Influence of rock fabric on fracture attribute distribution and implications for groundwater flow in the Nashoba terrane, eastern Massachusetts: *Journal of Structural Geology*, v. 30, no. 4, p. 464–477.
- Maniar, P.D., and Piccoli, P.M., 1989, Tectonic discrimination of granitoids: *Geological Society of America Bulletin*, v. 101, no. 5, p. 635–643.
- Manning, A.H., and de Boer, J.Z., 1989, Deformation of Mesozoic dikes in New England: *Geology*, v. 17, no. 11, p. 1016–1019.
- McKniff, J.M., 1964, *The petrology of the southern half of the Blackstone quadrangle, Massachusetts and Rhode Island*: Providence, Brown University, unpublished Master's thesis, scale 1:24,000, 74 p.

- O'Connor, J.T., 1965, A classification for quartz-rich igneous rocks based on feldspar ratios: U.S. Geological Survey Professional Paper 525-B, p. B79-B84.
- O'Hara, Kieran, and Gromet, L.P., 1985, Two distinct late Precambrian (Avalonian) terranes in southeastern New England and their late Paleozoic juxtaposition: *American Journal of Science*, v. 285, no. 8, p. 673-709.
- Passchier, C.W., and Trouw, R.A.J., 2005, *Microtectonics*: Berlin, Germany, Springer, 366 p.
- Pearce, J.A., Harris, N.B.W., and Tindle, A.G., 1984, Trace element discrimination diagrams for the tectonic interpretation of granitic rocks: *Journal of Petrology*, v. 25, no. 4, p. 956-983.
- Pearre, N.C., 1956, Mineral deposits and occurrences in Massachusetts and Rhode Island, exclusive of clay, sand and gravel, and peat: U.S. Geological Survey Mineral Investigations Resource Map MR-4, scale 1:500,000.
- Piazolo, Sandra, and Passchier, C.W., 2002, Controls on lineation development in low to medium grade shear zones; a study from the Cap de Creus Peninsula, NE Spain: *Journal of Structural Geology*, v. 24, no. 1, p. 25-44.
- Quinn, A.W., 1967, Bedrock geology of the Chepachet quadrangle, Providence County, Rhode Island: U.S. Geological Survey Bulletin 1241-G, p. G1-G26, 1 pl. in pocket, scale 1:24,000.
- Quinn, A.W., 1971, Bedrock geology of Rhode Island: U.S. Geological Survey Bulletin 1295, 68 p., 1 pl. in pocket, scale 1:125,000.
- Rast, Nicholas, and Skehan, J.W., 1990, The late Proterozoic geologic setting of the Boston Basin, *in* Socci, A.D., Skehan, J.W., and Smith, G.W., eds., *Geology of the composite Avalon terrane of southern New England*: Geological Society of America Special Paper 245, p. 235-247.
- Richmond, G.M., 1952, Bedrock geology of the Georgiaville quadrangle, Rhode Island: U.S. Geological Survey Geologic Quadrangle Map GQ-16, scale 1:31,680.
- Rowcroft, Jessica, and Doherty, Joanna, 2007, Uxbridge reconnaissance report, Blackstone Valley/Quinebaug-Shetucket Landscape Inventory, Massachusetts Heritage Landscape Inventory Program: Massachusetts Department of Conservation and Recreation, 49 p., <http://www.mass.gov/eea/docs/dcr/stewardship/histland/recon-reports/uxbridge-with-map.pdf>.
- Salvini, Francesco, 2010, DAISY 3; The Structural Data Integrated System Analyzer software (version 4.8.17): Rome, Italy, Università degli Studi di "Roma Tre," Dipartimento di Scienze Geologiche, software available at <http://host.uniroma3.it/progetti/fralab/Downloads/Programs/>.
- Salvini, Francesco, Billi, Andrea, and Wise, D.U., 1999, Strike-slip fault-propagation cleavage in carbonate rocks; the Mattinata fault zone, southern Apennines, Italy: *Journal of Structural Geology*, v. 21, no. 12, p. 1731-1749.
- Shand, S.J., 1951, *Eruptive rocks; their genesis, classification, and their relation to ore deposits* (4th ed.): New York, John Wiley & Sons, 488 p.
- Skehan, J.W., and Rast, Nicholas, 1990, Pre-Mesozoic evolution of Avalon terranes of southern New England, *in* Socci, A.D., Skehan, J.W., and Smith, G.W., eds., *Geology of the composite Avalon terrane of southern New England*: Geological Society of America Special Paper 245, p. 13-53.
- Skehan, J.W., and Rast, Nicholas, 1995, Late Proterozoic to Cambrian evolution of the Boston Avalon terrane, *in* Hibbard, J.P., van Staal, C.R., and Cawood, P.A., eds., *Current perspectives in the Appalachian-Caledonian orogen*: Geological Association of Canada Special Paper 41, p. 207-225.
- Spencer, E.W., and Kozak, S.J., 1976, Determination of regional fracture patterns in Precambrian rocks; a comparison of techniques, *in* Hodgson, R.A., Gay, S.P., Jr., and Benjamins, J.Y., eds., *Proceedings of the First International Conference on the New Basement Tectonics*, Salt Lake City, Utah, June 3-7, 1974: Utah Geological Association Publication 5, p. 409-415.
- Stone, B.D., Stone, J.R., and DiGiacomo-Cohen, M.L., comps., 2008, Surficial geologic map of the Worcester North-Oxford-Wrentham-Attleboro nine-quadrangle area in south-central Massachusetts: U.S. Geological Survey Open-File Report 2006-1260-D, <http://pubs.usgs.gov/of/2006/1260/D/>.
- Stroud, M.M., Markwort, R.J., and Hepburn, J.C., 2009, Refining temporal constraints on metamorphism in the Nashoba terrane, southeastern New England, through monazite dating: *Lithosphere*, v. 1, no. 6, p. 337-342, doi: 10.1130/L50.1.
- Sun, S.S., and McDonough, W.F., 1989, Chemical and isotopic systematics of oceanic basalts; implications for mantle composition and processes: *Geological Society Special Publications*, v. 42, p. 313-345.
- Thompson, M.D., Barr, S.M., and Grunow, A.M., 2012, Avalonian perspectives on Neoproterozoic paleogeography; evidence from Sm-Nd isotope geochemistry and detrital zircon geochronology in SE New England, U.S.A.: *Geological Society of America Bulletin*, v. 124, no. 3/4, p. 517-531, doi: 10.1130/B30529.1.

- Thompson, R.N., Morrison, M.A., Hendry, G.L., and Parry, S.J., 1984, An assessment of the relative roles of crust and mantle in magma genesis; an elemental approach: *Philosophical Transactions of the Royal Society of London*, v. A310, no. 1514, p. 549–590.
- Walsh, G.J., and Clark, S.F., Jr., 2000, Contrasting methods of fracture trend characterization in crystalline metamorphic and igneous rocks of the Windham quadrangle, New Hampshire: *Northeastern Geology and Environmental Sciences*, v. 22, no. 2, p. 109–120.
- Walsh, G.J., Aleinikoff, J.N., and Dorais, M.J., 2011, Bedrock geologic map of the Grafton quadrangle, Worcester County, Massachusetts: U.S. Geological Survey Scientific Investigations Map 3171, 1 sheet, scale 1:24,000, 39-p. text.
- Walsh, G.J., Aleinikoff, J.N., and Wintsch, R.P., 2007, Origin of the Lyme Dome and implications for the timing of multiple Alleghanian deformational and intrusive events in southern Connecticut: *American Journal of Science*, v. 307, no. 1, p. 168–215.
- Wayne, D.M., Sinha, A.K., and Hewitt, D.A., 1992, Differential response of zircon U-Pb isotopic systematics to metamorphism across a lithologic boundary; an example from the Hope Valley shear zone, southeastern Massachusetts, U.S.A.: *Contributions to Mineralogy and Petrology*, v. 109, no. 3, p. 408–420.
- Wintsch, R.P., and Aleinikoff, J.N., 1987, U-Pb isotopic and geologic evidence for late Paleozoic anatexis, deformation, and accretion of the late Proterozoic Avalon terrane, south central Connecticut: *American Journal of Science*, v. 287, no. 2, p. 107–126.
- Wintsch, R.P., and Sutter, J.F., 1986, A tectonic model for the late Paleozoic of southeastern New England: *Journal of Geology*, v. 94, no. 4, p. 459–472.
- Wintsch, R.P., Aleinikoff, J.N., Walsh, G.J., Bothner, W.A., Hussey, A.M., and Fanning, C.M., 2007, SHRIMP U-Pb evidence for a Late Silurian age of metasedimentary rocks in the Merrimack and Putnam-Nashoba terranes, eastern New England: *American Journal of Science*, v. 307, no. 1, p. 119–167.
- Wintsch, R.P., Coleman, M., Pulver, M., Byrne, T., Aleinikoff, J., Kunk, M., and Roden-Tice, M., 1998, Late Paleozoic deformation, metamorphism, and exhumation in central Connecticut, *in* New England Intercollegiate Geological Conference, 90th Annual Meeting, Kingston, R.I., Oct. 9–11, 1998, Guidebook to field trips in Rhode Island and adjacent regions of Connecticut and Massachusetts: Kingston, R.I., University of Rhode Island, p. C2-1–C2-21. (Edited by D.P. Murray.)
- Wintsch, R.P., Kunk, M.J., Cortesini, Henry, Jr., and Sutter, J.F., 1991, $^{40}\text{Ar}/^{39}\text{Ar}$ age-spectrum data for the Avalon and Putnam-Nashoba lithotectonic zones, eastern Connecticut and western Rhode Island: U.S. Geological Survey Open-File Report 91–399, 133 p.
- Wintsch, R.P., Sutter, J.F., Kunk, M.J., Aleinikoff, J.N., and Boyd, J.L., 1993, Alleghanian assembly of Proterozoic and Paleozoic lithotectonic terranes in south-central New England; new constraints from geochronology and petrology, *in* Cheney, J.T., and Hepburn, J.C., eds., Field trip guidebook for the northeastern United States: University of Massachusetts, Department of Geosciences, Geosciences Contribution 67, v. 1, p. H–1 to H–30. (Guidebook for the 1993 meeting in Boston of the Geological Society of America and the New England Intercollegiate Geological Conference.)
- Wintsch, R.P., Sutter, J.F., Kunk, M.J., Aleinikoff, J.N., and Dorais, M.J., 1992, Contrasting P-T-t paths; thermochronologic evidence for a late Paleozoic final assembly of the Avalon composite terrane in the New England Appalachians: *Tectonics*, v. 11, no. 3, p. 672–689.
- Wise, D.U., Funicello, Renato, Parotto, Maurizio, and Salvini, Francesco, 1985, Topographic lineament swarms; clues to their origin from domain analysis of Italy: *Geological Society of America Bulletin*, v. 96, no. 7, p. 952–967.
- Wones, D.R., and Goldsmith, Richard, 1991, Intrusive rocks of eastern Massachusetts, *in* Hatch, N.L., Jr., ed., The bedrock geology of Massachusetts: U.S. Geological Survey Professional Paper 1366 E–J, p. I1–I61.
- Zartman, R.E., and Hermes, O.D., 1987, Archean inheritance in zircon from late Paleozoic granites from the Avalon zone of southeastern New England; an African connection: *Earth and Planetary Science Letters*, v. 82, no. 3–4, p. 305–315.
- Zartman, R.E., and Naylor, R.S., 1984, Structural implications of some radiometric ages of igneous rocks in southeastern New England: *Geological Society of America Bulletin*, v. 95, no. 5, p. 522–539.
- Zartman, R.E., Hermes, O.D., and Pease, M.H., Jr., 1988, Zircon crystallization ages, and subsequent isotopic disturbance events, in gneissic rocks of eastern Connecticut and western Rhode Island: *American Journal of Science*, v. 288, no. 4, p. 376–402.
- Zen, E-an, ed., and Goldsmith, Richard, Ratcliffe, N.M., Robinson, Peter, and Stanley, R.S., comps., 1983, Bedrock geologic map of Massachusetts: Reston, Va., U.S. Geological Survey, 3 sheets, scale 1:250,000.

Manuscript approved on March 27, 2014

Prepared by the USGS Science Publishing Network
Publishing Service Centers

Edited by James R. Estabrook, Reston

Cartography and graphics by Linda M. Masonic, Reston

Layout by Caryl J. Wipperfurth, Raleigh

Web support by Angela E. Hall, Reston

For more information concerning this report, contact

Gregory J. Walsh

U.S. Geological Survey

P.O. Box 628

Montpelier, VT 05601

